SEISMIC HAZARD AND DESIGN SPECTRA AT
MILLSTONE NUCLEAR POWER PLANT,
UNIT 3

Dames & Moore

1626 Cole Blvd.
Golden, CO 80401
October 26, 1983

TABLE OF CONTENTS

1.0 INTRODUCTION

The purpose of this study is to make a probabilistic assessment of the frequency of exceedance of various ground acceleration levels and of the Safe Shutdown Earthquake (SSE) spectrum at the Millstone Nuclear Power Plant, Unit 3. This study looks at parameters and tectonic models originally examined in the Dames & Moore report prepared in January, 1983 in more detail. The results of the present study will be used to assess, in a general way, the relative frequency with which the SSE spectrum might be exceeded by earthquakes occurring in the northeastern U.S. The results on probabilities of exceedance of ground acceleration levels can be used to assess the probability of various damage levels for equipment and components in the plant as a result of earthquakes.

For this study, we rely heavily on our experience and judgment, both in guiding seismic hazard calculations and in drawing conclusions. The formal mathematical procedures used to calculate seismic hazard (described in Section 2) are standard ones for seismic hazard assessment of nuclear power plant safety, as documented in the TERA Corp. (1980) report of the Lawrence Livermore National Laboratory work, the USNRC Probabilistic Risk Assessment guide (American Nuclear Society, 1981), and the Indian Point Probabilistic Safety Study (IPPSS, 1982).

In addition to our own expertise, the work of TERA Corp. (1980) summarizes a wide range of opinion and expertise on seismicity in the central and eastern U.S. Other studies of eastern U.S. seismicity include Hadley and Devine (1974) and numerous other documents included in the list of references. The earthquake catalogs of Chiburis (1981) and the U.S. Geological Survey are the sources of historical earthquake data used here. Figure 1 shows the seismicity in the vicinity of Millstone reported in the Chiburis catalog. The U.S.G.S. catalog was used as the source of seismicity for states farther south.

Yankee Atomic Electric Company performed all of the computer analyses and computer plotting of results for this study. Dames & Moore was responsible for the general direction of the project and determined seismogenic zones, seismicity parameters, attenuation functions, and subjective weights for use in the computer analyses.

The specific facility examined in this study is the Millstone Nuclear Power Plant, Unit 3, New London County, Connecticut. The assumptions and hypotheses examined are appropriate for this site, but may not be for other sites. As an example, certain alternate configurations of seismogenic zones in the eastern U.S. may be appropriate for the evaluation of seismic hazard at other sites in the eastern U.S. These alternate configurations were not examined here because they would have no appreciable effect on the conclusions drawn for seismic hazard at the Millstone facility.

2.0 SEISMIC HAZARD MODEL

To develop probabilistic seismic hazard spectra at Millstone, it is possible to implement two procedures. The most direct would be to estimate spectral amplitudes at different frequencies directly, draw spectra corresponding to preselected frequencies of exceedance, and use these to compare to SSE spectra. However, because of the lack of strong motion data in the eastern U.S., the estimation of spectral amplitudes requires substantial judgment and is subject to criticism. The alternative is to estimate seismic hazard for acceleration and to anchor appropriate spectral shapes to these accelerations. This procedure has the advantage that numerous methods have been published to estimate acceleration in the eastern U.S., and spectral shapes can be derived from studies of west coast strong motion data. This second procedure is the one adopted for this study.

The seismic hazard model used in this study to estimate frequency-of-exceedance versus ground acceleration level has been described in detail elsewhere (Cornell, 1968, 1971; McGuire, 1976), and the steps involved are depicted in Figure 2. As shown in Figure 2a, the first step is to delineate zones of potential future earthquake occurrences, using seismicity, geology, and tectonic evidence. For each zone, data on historical earthquake occurrences are gathered, earthquake magnitudes are estimated from historical earthquake intensities using relationships proposed by Nuttli and Herrmann (1978) and by Weston Geophysical Corp. (1982). The data are plotted to indicate the number of earthquakes per unit time occurring in specific magnitude intervals, as illustrated in Figure 2b. A truncated exponential distribution is assumed to adequately represent the relative frequency of earthquake magnitudes in each zone, and the rate of earthquake occurrence is assumed to be accurately estimated by historical occurrences.

After delineating seismic zones and analyzing earthquake statistics, the third step is to adopt or derive an "attenuation function", shown in Figure 2c. This equation estimates peak acceleration as a function of earthquake magnitude

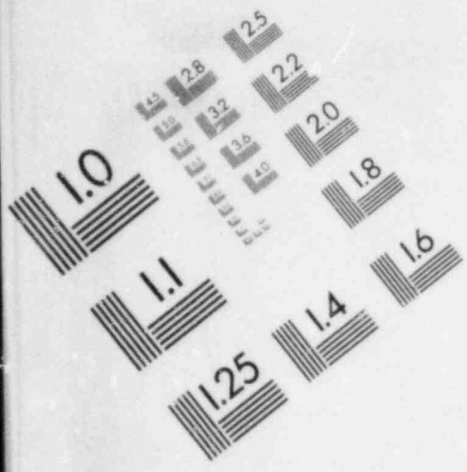

IMAGE EVALUATION TEST TARGET (MT-3)

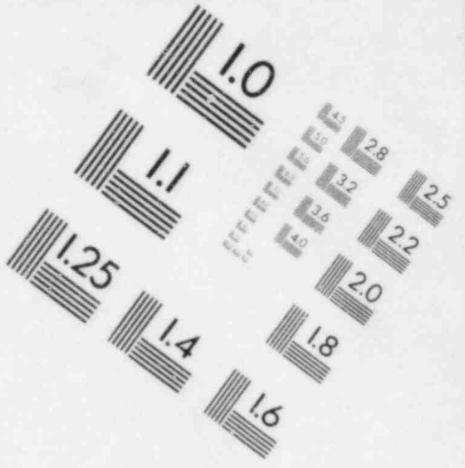

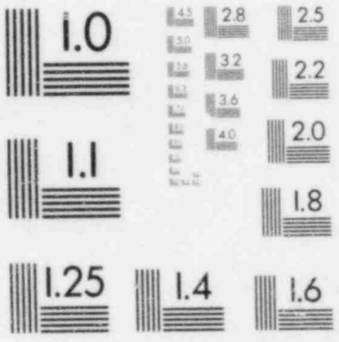

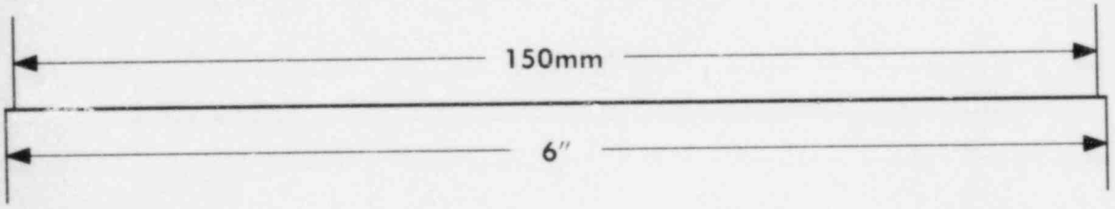

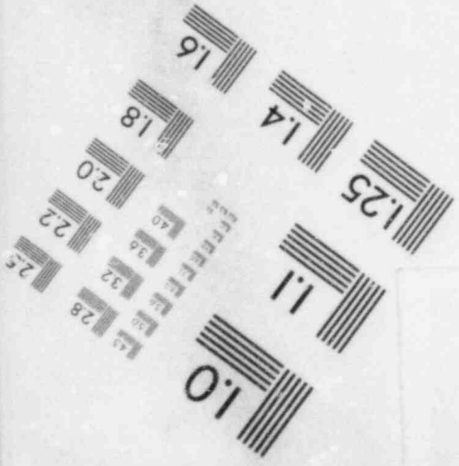

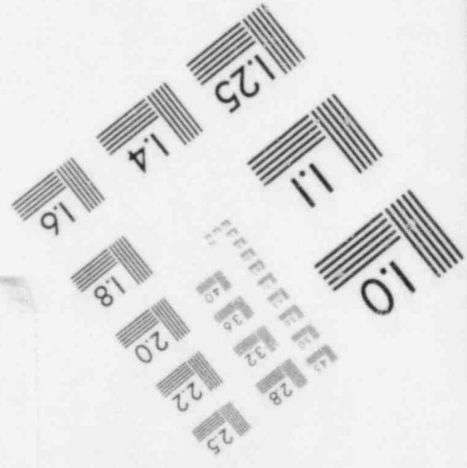

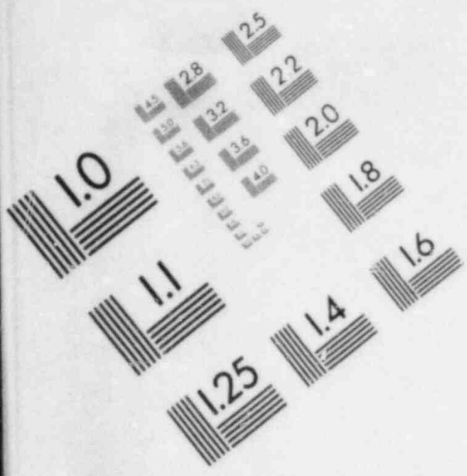

IMAGE EVALUATION TEST TARGET (MT-3)

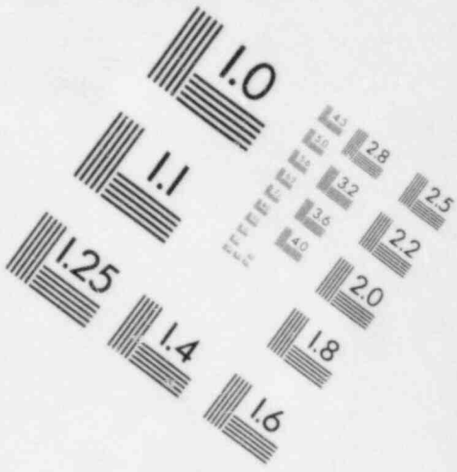

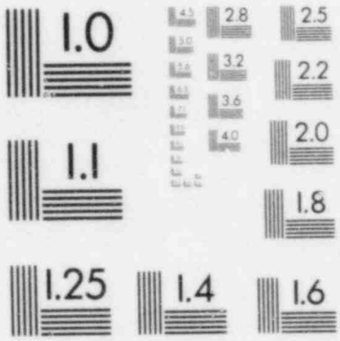

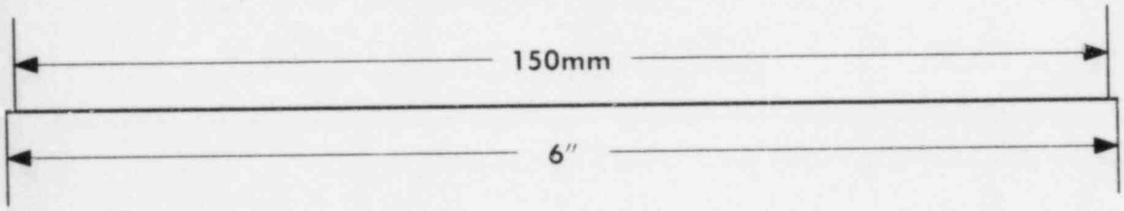

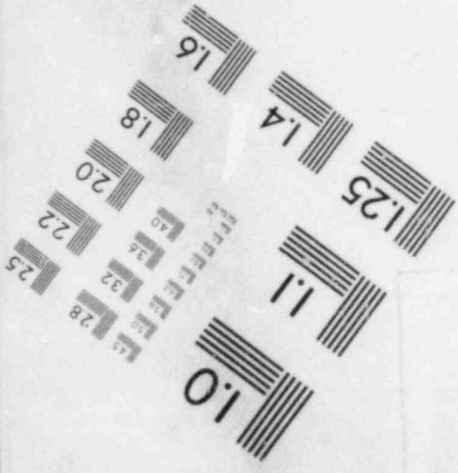

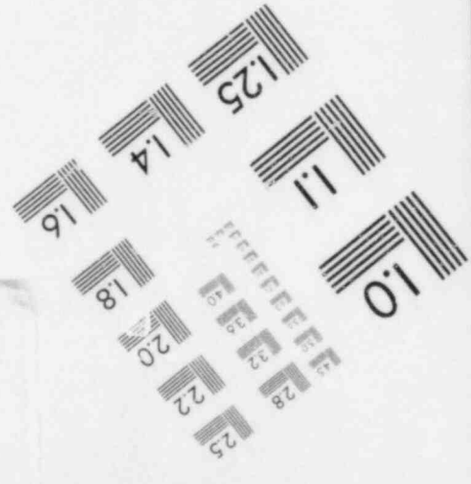

and distance between the source of seismic energy and the site. It is assumed that the peak acceleration predicted by the attenuation function is a median peak acceleration, and that actual values are lognormally distributed. The final step in the analysis consists of mathematically integrating over all possible earthquake magnitudes and locations, calculating for each magnitude and location the distribution of peak horizontal acceleration at the site to evaluate the annual frequencies that various levels of acceleration will be exceeded. A standard computer program (McGuire, 1976) is used for calculations. The output from this program is frequency of exceedance (number per unit time) as a function of peak acceleration which can be plotted as illustrated in Figure 2d.

Assumptions used in the seismic ground motion hazard analysis are listed in Table 1 for reference. The most basic assumptions are that seismogenic zones can be drawn to represent occurrences of future earthquakes, and that those occurrences can be represented probabilistically using the statistics of historical earthquakes in those zones. These assumptions, while quite gross, yield quite accurate estimates of seismic hazard (see, for example, McGuire, 1979, and McGuire and Barnhard, 1981). These are standard assumptions for seismic hazard analyses in regions where tectonic faults cannot be identified at the surface.

There are several assumptions required to describe seismicity within each seismogenic zone. First is that successive earthquakes are independent in time, location, and size. This means that the frequency of occurrence of an earthquake at a specific location in any year is not affected by seismicity (or lack of it) in prior years in the same general area. While this is physically unrealistic (any physical explanation of seismic events would account for the release of crustal stress, making future events at the same location unlikely in the short term), there are simply not enough data available in the short historical record to justify or calibrate more sophisticated models. Also, comparisons in areas where longer historical records are available indicate these assumptions are accurate if we are interested in estimating seismic hazard for periods on the order of 50 years (see the aforementioned refer-

be represented by a lognormal distribution with a logarithmic standard deviation of 0.6. Both assumptions are standard for this type of analysis, and are appropriate to characterize available earthquake ground motion data.

On balance, the assumptions used in seismic hazard analyses provide realistic estimates for the frequency of occurrence of peak ground acceleration. Not considered explicitly here are conservatisms associated with assuming that damage to structures is well-related to peak acceleration. This ground motion parameter is used here to anchor standard spectral shapes, not as a measure of earthquake-induced damage.

The spectral shapes anchored to accelerations developed by the above methodology are those derived by Bernreuter (1981) for magnitude 5.8 earthquakes. These spectra are shown in Figure 3. Events less than this magnitude, at distances of 24 to 49 km, generally dominate the seismic hazard for SSE-level ground motions. That is, if an exceedance of the SSE were to occur, it is likely to be caused by an earthquake with magnitude less than 5.8 at a distance of 24 to 49 km. Thus the representation of ground motion hazard with a magnitude 5.8 scaled spectrum is conservative but appropriate for the conclusions to be drawn in this study. This is discussed in more detail below.

ences). Finally, we observe that derived ground motion levels are not very sensitive to errors in frequencies of occurrence: an error in frequency of occurrence of a factor of two implies an error in ground motion amplitude of only thirty percent. Thus, we can mis-estimate earthquake frequencies by a large amount and only expect a relatively small error in the associated ground motion amplitude.

The typical probability distribution used to represent earthquake size is the double-truncated exponential distribution. This is an accurate representation of historical seismicity; its use to characterize future seismicity is appropriate if (as is the case in the eastern United States) no change in the character of tectonic strain accumulation or release is suspected. Parameters required to define this distribution are the lower bound, upper bound, and b-value. A lower-bound magnitude m_b of 4.5 was used in this study, based on the observation that earthquakes less than this size are not known to cause damage to engineered structures. In fact, this may be a conservative assumption: if, for example, seismic events in the range of 4.5 to 5.0 could also be shown to cause no damage, regardless of the peak accelerations generated, they should also be excluded from consideration. At present, such a demonstration is not possible quantitatively. The upper-bound magnitude is a realistic representation, based on all seismologic, geologic and geophysical data available. The method used in this study to examine the b-value is described below.

The random process used to represent earthquake occurrences in time is not critical to seismic hazard results. The levels of ground motion and their frequencies are such that only the mean rate of activity (number of earthquakes per year) is important. Thus the selection of a Poisson (or other) process does not seriously affect the results.

Other assumptions required in the analysis are that the peak acceleration can be represented as a function only of earthquake magnitude and source-to-site distance, and that the uncertainty in predicted peak acceleration can

3.0 SEISMOGENIC ZONES

The seismic hazard analysis requires the delineation of seismogenic zones, within which earthquakes are considered to be of similar tectonic origin so that future seismic events can be modeled by a single function describing earthquake occurrences in time, space, and size. Several sets of seismogenic zones were examined in this study, each set representing a different hypothesis on the structural and stress mechanisms causing earthquake occurrences in the vicinity of the site. These sets of seismogenic zones are discussed below.

3.1 GEOLOGIC PROVINCE ZONES

The Geological Province zones, shown in Figure 4, are based on a detailed investigation by Dames & Moore (1976) that formed the basis for direct testimony in the 1976 Show Cause Hearing about the Indian Point Site of Consolidated Edison Co. of New York. The zones in this model were developed on the basis of plate tectonic concepts; the zones outline those portions of the eastern United States affected by many overlapping periods of deformation, that could be differentiated on the basis of similarity in tectonic style and deformation. These zones were derived according to the NRC requirements for tectonic provinces (Appendix A to 10CFR, Part 100), and were successfully defended in public hearings as a valid design basis; they have relatively less credence than alternatives (because of the unclear association of current seismicity with Paleotectonic provinces) for the purpose of describing seismogenic zones for probabilistic seismic risk studies.

The Millstone site is in the Central New England Geologic Province zone. The largest historical earthquake in this zone was the m_b = 5.5 event which occurred on December 20, 1940 in New Hampshire.

3.2 TECTONIC PROVINCE ZONES

This model was developed by Hadley and Devine (1974) of the U.S. Geological Survey in conjunction with the U.S. Atomic Energy Commission (now NRC) as a means of introducing the concept of tectonic provinces and their relationship to earthquake occurrence in the eastern United States (see Figure 5). While basically similar to the Geologic Province model constructed by Dames & Moore, the Tectonic Province model is more generalized. For the purposes of this study, the Piedmont zone of Hadley and Devine (1974) was separated into a north and south Piedmont zone by dividing the original zone into two at Maryland. This is more representative of current scientific thinking on the extent of different effects in the northern and southern Piedmont during the various periods of divergent and convergent tectonism in the Piedmont.

The Tectonic Province zones provide the least detail and the most generalization; in a sense they are the lowest common denominator among alternatives based on crustal geology. The Millstone site lies within the northern Piedmont, but only about 30 km from the border of the Coastal Plain. The largest historical seismic shock in the northern Piedmont zone was the 1755 Cape Ann, Massachusetts, earthquake (estimated m_b = 5.8); the largest in the Coastal Plain is the 1886 Charleston, South Carolina, earthquake (estimated m_b = 6.6 to 6.8).

3.3 U.S. GEOLOGICAL SURVEY ZONES

The seismic zones drawn by Algermissen et al. (1982) (Figure 6) are used to represent seismicity for the U.S. Geological Survey model. These zones were derived using a combination of geological data, historical earthquake occurrences, and expert judgment, and represent one interpretation of tectonics.

The Millstone site lies near the boundary of USGS zone 103, which includes seismicity in western Connecticut, southern New York, and New Jersey, and USGS zone 107, which includes the Cape Ann seismicity. In the former, the largest

historical event was the 1884 Brooklyn earthquake (MM intensity VII, estimated m_b = 5.3). The largest Cape Ann earthquake was the 1755 event (MM intensity VIII, estimated m_b = 5.8). These two zones contribute about equally to the seismic hazard at Millstone.

3.4 NORTHERN APPALACHIAN ZONE

For this hypothesis, earthquakes in New York and New England are not assumed to be tied to identifiable structures in that region (Figure 7). Rather, it is assumed that seismic events are caused by as-yet-unidentified geologic features, and that these features may occur anywhere in the earth's crust. One large zone comprising the Appalachians and Piedmont province north of New Jersey is used to represent this model.

The Northern Appalachian zone is similar to the northern Piedmont of the Tectonic Province zones, and is examined separately here because it represents one zone considered reasonable by the NRC (Policy Issue memo from Dircks to Commissioners dated February 5, 1982). The largest historical earthquake in the Northern Appalachian zone was the 1755 Cape Ann event (maximum intensity VIII).

3.5 DECOLLEMENT ZONE

This model hypothesizes that a crustal zone in the eastern United States is undergoing horizontal movements (Seeber and Armbruster, 1981). Large scale overthrusting has been inferred to occur from the New England Appalachians and perhaps even farther west. Movement is either consistent with overthrust of the crust (to the west) or backsliding (to the east) due to gravity.

In addition, Behrendt et al. (1980) have interpreted northeast striking low-angle thrust faults at depths of 10 to 15 km near the Charleston S.C. area. These depths are in the range of hypocentral depths for a cluster of recent earthquakes (1973-1978). It has been inferred that this low-angle thrust coincides with the Decollement identified in the COCORP profiles. Earthquakes

in the Decollement model (up to $m_{b,max}$ of 7.0) are inferred, therefore, to occur along the horizontal detached zone similar to the discussion by Behrendt, et al. (1980) for the Charleston 1886 event.

Because the eastern border of the Decollement zone, which is drawn at the boundary between the Central New England Province and the craton, is not well defined, two versions of the model have been considered here. The first version is shown on Figure 8. The Millstone site lies outside of the zone in this version, but within the zone considered as background. The Millstone site lies inside the Decollement Zone in Version 2 (Figure 9).

The Decollement model itself has not received much support as an explanation for earthquakes in the eastern U.S. While the existence of the detached surface is considered quite possible by many researchers, the conclusion that movement on this surface causes earthquakes, or that the detachment exists as a single widespread surface throughout the Appalachian Orogen, is not held except by a few. The model is a useful one to illustrate the implied hazard if Charleston-size earthquakes are assumed to be possible anywhere on the east coast.

3.6 MESOZOIC RIFT ZONES

This model combines the arguments posed by Diment et al. (1980) with those of Wentworth et al. (1981). Earthquakes are assumed to occur in northeast-trending Mesozoic rift basins where they terminate northwest-trending crustal block boundaries. The rift basins are considered to represent the margin of crustal divergence after the last opening of the Atlantic. Earthquakes within the basins are inferred to occur along re-activated border faults of Mesozoic origin, similar to the argument posited by Wentworth et al. (1981). The Ramapo fault in New York is thought to be one example of a Mesozic Basin border fault, although there is controversy over the relationship of this fault to earthquakes.

Two versions of this model were considered here because of the uncertainty in the boundaries of the rift basins. Version 1 (Figure 10) is the case where the site lies outside of the Connecticut Valley Rift structure. Version 2 (Figure 11) is the case where the site lies inside this structure. The maximum historical event in the Connecticut Valley Rift zone is the 1884 Brooklyn earthquake (MM intensity VII, estimated m_b = 5.3).

3.7 MESOZOIC INTERSECTION ZONES

Earthquake occurrences for this model are assumed to be controlled by the intersection of Mesozoic rift basins and northwest-trending crustal features. Most of these inferred features cross rift basins at their northeast or southwest limits. These zones have necessarily been drawn in a broad fashion to reflect uncertainty in the location of these features and in the epicentral location of historical seismicity.

The development of the scientific basis for these zones has been relatively recent, although the idea of intersecting structures causing large earthquakes is not new. Such a structure is one proposed explanation of the Charleston earthquake.

The intersection zones representing seismicity in Connecticut and southern New York are inferred from offshore fracture zones and indirect gravity and magnetic data. Therefore these two zones are conjectural; they have been included in the hazard calculations as one possible interpretation of tectonics in the northeast, with an associated small confidence level. However, because the site lies near the Connecticut intersection zone, two versions of this model were considered. In the first version (Figure 12), the site lies outside the Connecticut Intersection zone, but inside the area considered background. In the second version (Figure 13), the site lies inside the Connecticut Intersection zone. The largest historical event in this zone is the 1791 Moodus, Connecticut earthquake (MM intensity = VI, estimated m_b = 4.8).

3.8 MAFIC PLUTON ZONES

This set of zones reflects the hypothesis that earthquakes are associated with mafic plutons chiefly of Paleozoic age. These mafic plutons occur over regions in northern New England, as shown in Figure 14 (from The Final Safety Analysis Report for Millstone Nuclear Power Station, Unit 3). Because the site lies more than 180 km from these zones, this seismogenic model effectively acts to restrict large earthquakes to locations far from Millstone.

The largest historical earthquake in the closest zone (White Mountains Pluton Zone) is the 1755 Cape Ann event (MM intensity VIII, estimated m_b = 5.8). The site lies in the area considered background.

3.9 SUBJECTIVE WEIGHTS ON ZONES

For the purpose of deriving the relative likelihood associated with hazard curves, subjective weights were assigned to the sets of seismogenic zones described above. These weights reflect the subjective judgment that each set of zones is the correct one for describing seismic hazard.

The subjective weights were judged to be equally-likely for two categories of zones, and each category was assigned a weight of 0.50. The first category represents zonations based, in part, on crustal geology, and includes the Geologic Province zones, the Tectonic Province zones, and the U.S. Geological Survey zones. Within this category, the Tectonic Provinces zones were considered somewhat more likely. in that they are broader and were drawn using historical seismicity. They do not consider the Ramapo fault as a possible source of large earthquakes, a possibility which is currently unresolved but appears unlikely. This model was weighted 0.25. The Geologic Province zones were judged to be least likely, because they account only for geology and do not consider seismicity. This model was weight 0.10. The U.S. Geological Survey zones, based on geology and seismicity, were assigned a weight of 0.15.

The second category of seismogenic zonations includes the Northern Appalachian zone, Mesozoic Rift zones, Mesozoic Intersection zones, the Decollement zone and Mafic Pluton zones. Within this category, the Mesozoic Rift zones were assigned a weight of 0.10. The Mesozoic Intersection zones, Decollement zone, and Mafic Pluton zones were considered unlikely and were assigned a weight of 0.05 each. The Mesozoic Intersection zones and Decollement zone are presently questioned as to their validity in the Millstone area. The Mafic Pluton zones have no effect on Millstone because of their distance from the site. For all three of these models, the background contributes equally or greater to the seismic risk at the Millstone site than the modeled zones themselves. Therefore, these models are more aptly described by the Northern Appalachian zone, which treats seismicity as a broad, diffuse zone; this zone was assigned a weight of 0.25.

The subjective weights assigned to each set of seismogenic zones are summarized as follows:

Geologic Province zones	0.10
Tectonic Province zones	0.25
U.S. Geological Survey zones	0.15
Northern Appalachian zone	0.25
Decollement zone, Versions 1 & 2	0.05
Mesozoic Rift zones, Versions 1 & 2	0.10
Mesozoic Intersection zones, Versions 1 & 2	0.05
Mafic Pluton zones	0.05
TOTAL	1.00

For zones represented by two versions with Millstone inside and outside the dominant zone (the Mesozoic Rift, Mesozoic Intersection, and Decollement zones), the weight shown was divided equally between the two versions. There is no one set of zones which stands out as being overwhelmingly credible. The final results to be presented are not heavily dependent on the exact weights assigned. The eleven sets of zones in Figures 4 through 14 represent the range

of possible seismogenic zone interpretations in the northeastern U.S., and represent a reasonable range of hypotheses with which to investigate seismic hazard at the Millstone Nuclear Power Station.

4.0 SEISMICITY PARAMETERS

For the probabilistic calculation of seismic hazard, several parameters describing seismicity are required for each seismogenic zone. These parameters, and the methods used to estimate mean values and to quantify uncertainty, are discussed below. The Chiburis (1981) catalog of historical earthquakes was used as the data base for New England, Canada, and east central U.S. The U.S. Geological Survey data base (published as state seismicity maps, for example Reagor et al., 1980) was used for the southeastern U.S. and was updated with data of Bollinger and Sibol (1983), and Dewey and Gordon (written communication, 1983). Listed in Appendix A are all earthquakes in the catalog within 322 km (200 miles) of the site, with MM intensity greater than or equal to V. For statistical data analysis, earthquakes with an epicentral MM intensity I_e but without a magnitude estimate (pre-instrumental seismicity) were converted to a body-wave magnitude m_b using the two relationships:

$$m_b = 1.75 + 0.5\ I_e \qquad (1)$$

$$m_b = 0.44 + 0.67\ I_e \qquad (2)$$

Equation 1 was derived for the central U.S. (Nuttli and Herrmann, 1978) and is considered reliable for the eastern U.S. as well (Bollinger, personal communication, 1983). The second equation was derived using New England data (Weston Geophysical Corp., 1982), and is considered a reasonable alternative.

4.1 RICHTER b-VALUE

The Richter b-value describes the slope of the log-number versus magnitude relation:

$$\log_{10} n(m_b) = a - bm_b \qquad (3)$$

where $n(m_b)$ is the annual number of earthquakes of body-wave magnitude m_b, and a and b are parameters fit to seismicity data. Parameter a is related to the seismic activity rate as discussed in Section 4.2.

Two values of b in equation 3 were calculated from historical earthquakes using the following procedure. Magnitudes, when not reported instrumentally, were estimated from MM intensities using first, equation 1 and second, equation 2, and the number of events per decade were counted into magnitude intervals centered on magnitudes estimated from even MM intensity values. Periods of historical completeness were determined in a manner designed to give the highest observed rate of occurrence. These periods were generally as follows:

Magnitude (m_b) (Equation 1)	Magnitude (m_b) (Equation 2)	MM Intensity	Period
3.8	3.1	IV	1970-present
4.3	3.8	V	1950-present
4.8	4.5	VI	1900-present
5.3	5.1	VII	1720-present
5.8	5.8	VIII	1720-present
6.3	6.5	IX	1720-present
6.8	7.1	X	1660-present

For each zone and for each method of converting from intensity to magnitude, the number of events in each magnitude interval was used as data and a b-value and its uncertainty were determined using the maximum likelihood method (Weichert, 1980).

Uncertainty in the method of calculating the Richter b-value was incorporated in the hazard calculations by using each of the two conversion methods (equation 1 and equation 2), and weighting each equally (with a weight of 0.5). Further, uncertainty in the b-value given the method of calculation was examined by changing the b-values by $\pm$ 15 percent in conjunction with the changes in maximum magnitude described below. This change reflects statistical uncertainty in the b-value, given its chosen method of calculation; 15 percent is a typical one-standard-deviation uncertainty in b-value as determined by the method of Weichert (1980). Probabilities associated with these changes in b-value are discussed below in the section on maximum magnitude.

4.2 SEISMIC ACTIVITY RATE

The rate of earthquake occurrence was determined for each seismogenic zone and for each intensity-to-magnitude conversion equation by the maximum likelihood method (Weichert, 1980), using as data the historical earthquakes in that zone. Activity rates were calculated for occurrences of earthquakes with $m_b \geq 4.5$, (where m_b is body-wave magnitude) which corresponds to MM intensity V-VI. This method was based on the observation that earthquakes of smaller magnitude rarely cause structural damage, even if peak accelerations are high, due to the short duration, impulsive-type ground motions associated with these small events. No uncertainty in activity rates was considered herein, because historical rates of seismic activity are relatively well-determined, even in the eastern U.S. (McGuire, 1977). Important in this assumption is the consideration that calculated frequencies of exceedance are directly proportional to activity rates, and ground motion amplitudes at levels of interest change relatively slowly with respect to frequency of exceedance.

4.3 MAXIMUM MAGNITUDE

For the Geologic Provinces, Tectonic Provinces, U.S. Geological Survey zones, and Northern Appalachian zone, the best estimate of maximum possible magnitude $m_{b,max}$ in each zone was taken to be 0.5 magnitude units above the magnitude of the largest historical earthquake. This corresponds to approximately one MM intensity unit higher than the maximum historical MM intensity, and is consistent with, for example, a concensus of the experts polled in the TERA Corp. (1980) study. The only exception among these zones was for the Coastal Plain zone of the Tectonic Provinces, where the 1886 Charleston earthquake occurred and where $m_{b,max} = 7.0$ was assumed.

For the Decollement zone, the value of $m_{b,max}$ was chosen to be 7.0, consistent with the occurrence of the 1886 Charleston earthquake in that zone (estimated $m_{b,max} = 6.8$). For the Mesozoic Rift zones and the Mesozoic

Intersection zones, two values of $m_{b,max}$ (6.0 and 7.0) were used to express uncertainty in the values for these zones. The $m_{b,max}$ was not varied for the Mafic Pluton zones because the background dominates the seismic hazard.

For zones where the best estimate of $m_{b,max}$ was taken to be the maximum historical magnitude + 0.5, alternative values of $\pm$ 0.5 magnitude units from the best estimate were examined to determine the effect of uncertainty in maximum magnitude on the hazard calculations. The three values of maximum magnitude were weighted equally (i.e., one-third each). In the hazard calculations, it was assumed that uncertainty in maximum magnitude was perfectly correlated with statistical uncertainty in the Richter b-value (described above). The reason is that there is some suspected negative correlation between these two variables (small b-values tend to correlate with high maximum magnitudes, and vice versa). An accurate modeling of this negative correlation is beyond the level of sophistication required for this study; an assumption of perfect negative correlation gives accurate results in the mean and, if anything, over-emphasizes the effect sought. In the case of the Mesozoic Rift and Mesozoic Intersection zones (in which $m_{b,max}$ was varied between 6.0 and 7.0), the b-value was not varied. The lower value of maximum magnitude was assigned a weight of 0.8, while the higher value was assigned 0.2.

Table 2 presents the eleven hypotheses on seismogenic zones considered. Seismicity parameters are shown for the zone which dominates seismic hazard, for each hypothesis. In all cases, all zones shown in Figures 4 through 14 were used in the hazard calculations to confirm that only the most active zone closest to the site contributed to seismic hazard.

5.0 ESTIMATION OF SEISMIC GROUND MOTION

Estimates of peak single-component horizontal ground acceleration, a_p, were made for this study using four methods. These are described in the following paragraphs.

The first attenuation equation used is that of Nuttli and Herrmann (1981):

$$\ln a_p = 1.265 + 1.15\, m_b - 0.0044\, \Delta - 0.833 \ln \Delta \qquad (4)$$

where Δ is epicentral distance and a_p is in cm/sec^2. This function is plotted in Figure 15. For any given magnitude, accelerations in the near-field are assumed to be constant (see the horizontal portion of the curves shown in Figure 15) and limited as a function of magnitude by the following relationship (Nuttli and Herrmann, 1981):

$$\ln a_p\,(max) = 0.933\, m_b \qquad (5)$$

The attenuation function published by Campbell (1981a) for stiff soil and rock sites in the central U.S. was also used in this study:

$$\ln a_p = -4.39 + .922M - 1.27 \ln (\Delta + 25.7) - \gamma\Delta \qquad (6)$$

where

$$\gamma = 0.023 - 0.0048M + 0.00028\, M^2 \qquad (7)$$

and where M is moment magnitude, essentially equivalent to local magnitude for the range of interest in this study (magnitudes less than 7). Moment magnitude was converted to body wave magnitude (the scale used in this study to characterize earthquakes) by the relation (Campbell, 1981a):

$$M = 1.02\ m_b + 0.30 \qquad m_b < 5.6 \qquad (8)$$
$$M = 1.64\ m_b - 3.16 \qquad m_b \geq 5.6$$

Equation 6 was assumed to apply for all distances, and is plotted in Figure 16. This equation and the Nuttli-Herrmann attenuation function (equation 4) were derived primarily for the central U.S., and are adopted here as two estimates of ground motion for the northeastern U.S.

Two additional attenuation equations were derived from MM intensity attenuation observed during earthquakes in New England (G. Klimkiewicz, personal communication, 1982). This intensity attenuation is:

$$I_s = -1.43 + 1.79\ m_b - 0.80\ \ln \Delta - 0.00184\ \Delta \qquad (9)$$

where I_s is MM intensity at a site located epicentral distance Δ from the earthquake. Two methods of converting I_s to a_p were used (McGuire, 1977):

$$\ln a_p = 0.831 + 0.851\ I_s \qquad (10)$$

$$\ln a_p = 1.45 - 0.359\ \ln \Delta + 0.68\ I_s \qquad (11)$$

The first of these equations represents a one-to-one transformation between site intensity and peak acceleration; the second recognizes that this transformation may be a function of epicentral distance. Equations 10 and 11 were derived for stiff soil sites and are assumed here to apply to rock sites as well. Substituting equation 9 into 10 and 11 gives:

$$\ln a_p = -2.05 + 1.523\ m_b - 0.68\ \ln \Delta - 0.00157\ \Delta \qquad (12)$$

$$\ln a_p = 0.478 + 1.22\ m_b - 0.90\ \ln \Delta - 0.00125\ \Delta \qquad (13)$$

The first of these is herein designated the "AI" ("Acceleration from Intensity") attenuation; the second is designated the "AID" ("Acceleration from Intensity with Distance-dependence") attenuation. These two functions are plotted in Figures 17 and 18, respectively.

In this study, all four attenuation equations were used. For the purposes of deriving best-estimate and fractile hazard curves, a subjective weight of one-fourth was used with each attenuation function (equations 4, 6, 12, and 13).

For calculations of seismic hazard, a lognormal distribution of acceleration about the mean value was assumed, with a value of $\sigma_{\ln a}$ equal to 0.6, corresponding to a factor of 1.8 uncertainty in the estimate. This distribution is widely used to represent uncertainty in ground motion estimates. The uncertainty modeled is typical of the scatter exhibited by strong motion data sets, as shown in Table 3, when the data are restricted to a specific area such as the western U.S. Data from a specific earthquake may show a standard deviation less than 0.6 (for example, the Donovan study of the San Fernando earthquake), but this is only representative of that one event. When data from worldwide locations are used in the analysis, larger values of uncertainty are obtained because of different mean attenuations. In this study it is more appropriate to use an uncertainty typical of a specific geographic area.

The distribution of peak ground acceleration was truncated, to reflect the notion that, if MM intensities are limited, so must peak accelerations be limited. Whether or not instrumental peak accelerations are limited is problematic; the idea is that, if damage from earthquakes is bounded in a region, the effective ground motion must also be bounded. The bounds used in this analysis are shown in Table 4.

The third column of Table 4 shows upper bound values of sustained acceleration, where this corresponds to the third highest peak. These upper bound values for MM intensity VI, VII, VIII, and IX were obtained from Kennedy (personal communication, 1981). The values of sustained acceleration shown in

Table 4 for half values of MM intensity were derived by observing that a decrease of sustained acceleration of 20 percent for each half intensity unit is consistent with the limits suggested by Kennedy. These limits on sustained acceleration must be multiplied by the factor 1.25 to convert to a peak acceleration. The basis for this factor is experience with the relationship between sustained ground motion which causes damage by several cycles of induced motion, and the associated peak acceleration for earthquakes of large enough magnitude (>6) to cause long durations of strong shaking (Kennedy, personal communication, 1981).

These limits were applied to all calculations of seismic hazard in this study. For example, in the numerical integration over magnitude, the occurrence of magnitude 6 (corresponding to MM intensity VIII-IX) implies that the resulting distribution of peak accelerations was truncated at 0.8 g, as shown in Table 4. If $m_{b,max}$ is 6 for the zone dominating hazard at Millstone, the calculated annual frequencies of exceedance of peak accelerations greater than 0.8 g is zero.

6.0 RESULTS OF ANALYSIS

Figure 19 shows the calculated annual frequency of exceedance for the Northern Appalachian zone using the Weston conversion, for the four attenuation equations. The AI and AID attenuation equations indicate approximately the same hazard. For accelerations greater than 100 cm/sec^2, the Nuttli-Herrmann and the Campbell attenuation equations indicate approximately three times higher hazard than the AI and AID equations.

The sensitivity of hazard to the choice of seismogenic zonation is shown in Figure 20. Using the Nuttli-Herrmann conversion and attenuation equation, the total range in hazard (frequency for a given acceleration) is about a factor of ten for the range of seismogenic zones at an acceleration of 100 cm/sec^2 and increases at higher accelerations.

The sensitivity of hazard from version 1 (site outside the designated zone) to version 2 (site inside the designated zone) in the case of the Decollement Zone, is shown in Figure 21. The curves shown represent results using the Nuttli-Herrmann conversion, and both the Nuttli-Herrmann and AID attenuation equations. In both cases, version 1 is higher than version 2 by a factor of about two, because the activity rate in the background area (Figure 8) exceeds that in the Decollement zone (Figure 9).

Seismic hazard curves as a function of maximum magnitude ($m_{b,max}$) are shown in Figure 22. The curves shown are for the Northern Appalachian zone, using both the Nuttli-Herrmann and Weston conversions and the Nuttli-Herrmann attenuation. The uncertainty in $m_{b,max}$ (and simultaneous statistical uncertainty in the b-value, as described in Section 4.3 of this report) translates into uncertainty of $\pm$ a factor of two in annual frequency, from the best-estimate value of $m_{b,max}$.

Figure 23 shows the effect of the method used to convert intensity to magnitude. The curves for both the Nuttli-Herrmann and the Weston conversions are shown for the Northern Appalachian zone using the Nuttli-Herrmann and AID attenuation equations. The difference between the two conversions is about a factor of two at accelerations greater than 100 cm/sec^2.

In all, 184 seismic hazard curves were generated in this study: eleven sets of seismogenic zones times four attenuation functions, times two methods of converting intensity to magnitude, times three maximum magnitudes (two in the cases of Rift and Intersection Zones and one in the cases of Decollement and Pluton zones). To synthesize and present these results, the curves were aggregated into ten representative curves. Details of the aggregation procedure are discussed in Yankee Atomic Electric Co. (1982). One modification of this procedure was made, to ensure that all original hazard curves with truncations of about 0.6 g (see Table 4) were aggregated together and not mixed with curves with a higher truncation. The same procedure was followed for curves truncated at about 0.8 g, and at about 1.0 g and greater. Figure 24 shows the ten aggregate hazard curves; Figure 25 shows the median, 16% and 84% fractile curves. These two figures give an indication of the uncertainty in the hazard as a result of the combined uncertainty in seismogenic zones, attenuation functions, maximum magnitudes, and intensity-magnitude conversions. From the sensitivities shown in Figures 19 through 23, no single uncertainty in input dominates the uncertainty in seismic hazard.

Seismic hazard results for the ten aggregate curves are given in Table 5, in terms of annual frequencies of exceedance for various peak accelerations. As a result of the aggregation procedure, three curves are truncated at 0.6 g, three are truncated at 0.8 g, and four are untruncated. (The untruncated aggregate curves each represent several hazard curves which are truncated at 1 g and several which are not.) Also shown on Table 5 is the probability associated with each curve, which is the combined probability of the original hazard curves represented by each aggregate curve.

For all hazard calculations the average magnitude causing exceedances of each acceleration level was calculated using the procedure described in McGuire and Shedlock (1981). These indicated that, for accelerations around 0.17 g, magnitudes around 5.6 dominate the hazard (the average magnitude ranged from 5.2 to 5.9, depending on the source area). The average distance at which these events occurred ranged from 24 to 49 km, with the closer distances associated with smaller average magnitudes and the larger distances with higher average magnitudes. Thus the results should not be interpreted to mean that the SSE will be caused by a magnitude 5.6 in the near-field; if such an event causes an exceedance of the SSE, it will most likely occur at 30 to 50 km. The choice of a magnitude 5.8 spectrum is made merely to obtain a conservative spectral shape which, when anchored to the peak acceleration, will give a general indication of the response spectrum associated with these events.

Figure 26 shows the Bernreuter (1981) spectrum (5% damping) of Figure 3 scaled to the 10^{-3} and 10^{-4} acceleration levels for the median curve shown in Figure 25. Also shown is the SSE spectrum for 5% damping for Millstone Unit 3. The latter spectrum lies approximately at the 10^{-4} level (or lower) throughout the frequency range 25 to 1 hz.

7.0 SUMMARY

We present here a seismic hazard analysis for peak ground acceleration at the Millstone Nuclear Power Plant, Unit 3. The analysis is primarily dependent on the spatial extent of any hypothesized seismic source which produces earthquakes in the vicinity of the site, on the method of converting intensity to magnitude, on the attenuation equation used, and on the maximum magnitudes assumed. This is illustrated by the sensitivity of calculated seismic hazard shown in Figures 19 through 23. For the purposes of reporting, ten aggregate curves are obtained; these aggregate curves illustrate the range and uncertainty in results obtained from uncertainties in seismicity and attenuation.

The acceleration hazard at the SSE level (0.17 g) is represented by a frequency of exceedance of approximately 10^{-4} per year, and is dominated by earthquakes with a mean magnitude in the range 5.2 to 5.9. A site-specific, magnitude 5.8 near-source spectrum anchored to the peak accelerations indicates that the SSE spectrum for Millstone Unit 3 lies at about the 10^{-4} frequency-of-exceedance level throughout the frequency range of engineering interest.

REFERENCES

Algermissen, S.T., D.M. Perkins, P.C. Thenhaus, S.L. Hanson, and B.L. Bender (1982), "Probabilistic Estimates of Maximum Acceleration and Velocity in Rock in the Contiguous United States", U.S.G.S. Open-File Report 82-1033, 99 pp.

American Nuclear Society (1981), "PRA Procedures Guide," USNRC, NUREG/CR-2300.

Behrendt, J.C., R.M. Hamilton, H.D. Ackermann, J.V. Henry, and K.C. Bayer, (1980) "Seismic Reflection Evidence of Cenozoic Reactivation of Older Faults on Land and Offshore in the area of Charleston, South Carolina 1886 Earthquake", GSA, Vol. 12, No. 7, ABS., 93rd An. Mtg, Atlanta, Georgia.

Bernreuter, D.L. (1981), C.P. Mortgat, and L.H. Wright (1979), "Seismic Hazard Analysis: Site Specific Response Spectra Results", prepared for TERA Corp.

Bollinger, G.A., and M.S. Sibol (1983), "Listing of Hypocenters from Southeastern U.S. Seismic Network", Virg. Poly. Inst. and State Univ., Bull. No. 10A, April.

Campbell, K.W. (1981a), "A Ground Motion Model for the Central United States Based on Near-Source Acceleration Data", Proc., Earthquakes and Earthquake Eng.: The Eastern U.S., Knoxville, Sept., pp. 213-232.

Campbell, K.W. (1981b), "Near Source Attenuation of Peak Horizontal Acceleration", Bull. Seis. Soc. Am., Vol. 71, No. 6, p 2039-2070.

Chiburis, E. (1981), "Seismicity, Recurrence Rates, and Regionalization of the Northeastern United States and Adjacent Southeastern Canada", USNRC, NUREG/CR-2309.

Cornell, C.A. (1968), "Engineering Seismic Risk Analysis", Bull. Seis. Soc. Am., Vol. 58, p. 1583-1606.

Cornell, C.A. (1971), "Probabilistic Analysis of Damage to Structures under Seismic Load", Chapter 27 in Dynamic Waves in Civil Engineering, D.A. Howells, I.P. Haigh, and C. Taylor, Editors, Wiley Interscience, London, p. 473-488.

Cornell, C.A., H. Banon, and A.F. Shakal (1979), "Seismic Motion and Response Prediction Alternatives", Earthquake Eng. and Struc. Dyn., Vol. 7, p. 295-315.

REFERENCES (Continued)

Dames & Moore (1976), Testimony before the Atomic Safety and Licensing Appeal Board in the matter of the Citizen's Committee on Protecting the Environment vs. Consolidated Edison of New York, Inc., and the Power Authority of the State of New York, Issue 1, Tectonic Provinces (April).

Dimert, W.H., O.H. Muller, and P.M. Lavin, (1980), Basement Tectonics of New York and Pennsylvania as Revealed by Gravity and Magnetic Studies, Proc., "The Caledonides in the U.S.A.", L.G.C.P. Project 27, Caledonide Orogen, p. 221-227.

Donovan, N.C. (1973), "Earthquake Hazards for Buildings", in Building Practices for Disaster Mitigation, Natl. Bur. Standards Building Sc. Series 46, p. 82-111.

Donovan, N.C. (1974), "A Statistical Evaluation of Strong Motion Data Including the February 9, 1971 San Fernando Earthquake", Proc., 5th World Conf. on Earthquake Eng., Rome, Vol. 1. p. 1252-1261.

Esteva, L., and R. Villaverde (1974), "Seismic Risk, Design Spectra, and Structural Reliability", Proc., 5th World Conf. on Earthquake Eng., Rome Vol.2, p. 2586-2596.

Hadley, J.B., and J.F. Devine (1974), "Seismotectonic Map of the Eastern United States", Department of the Interior, U.S.G.S., Misc. Field Studies Map MF-620.

IPPSS (1982), "Indian Point Probabilistic Safety Study," Con. Ed. of N.Y. and Power Auth. of the State of N.Y., Docket Nos. 50-247-SP and 50-286-SP.

Joyner, W.B., and D.M. Boore (1981), "Peak Horizontal Acceleration and Velocity from Strong Motion Records Including Records from the 1979 Imperial Valley, California, Earthquake", Bull. Seis. Soc. Am., Vol. 71, No. 6, p 2011-2038.

McGuire, R.K. (1974), "Seismic Structural Response Risk Analysis, Incorporating Peak Response Regressions on Earthquake Magnitude and Distance", Massachusetts Inst. Technology, Dept. Civil Eng., Research Rept. R74-51, p. 371.

McGuire, R.K. (1976), "Fortran Computer Program for Seismic Risk Analysis", U.S.G.S., Open-File Report 76-67.

REFERENCES (Continued)

McGuire, R.K. (1977), "Effects of Uncertainty in Seismicity on Estimates of Seismic Hazard for the East Coast of the United States", Bull. Seis. Soc. Am., Vol. 67, No. 3., June, p 827-848.

McGuire, R.K. (1978a), "Seismic Ground Motion Parameter Relations", Jour., Geotech. Eng. Div., A.S.C.E., April, p 481-490.

McGuire, R.K. (1978b), "A Simple Model for Estimating Fourier Amplitude Spectra of Horizontal Ground Acceleration", Bull. Seis. Soc. Am., Vol. 68, No. 3, June, p 803-822.

McGuire, R.K. (1979), Adequacy of Simple Probability Models for Calculating Felt-Shaking Hazard Using the Chinese Earthquake Catalog. Bull. Seis. Soc. Am., Vol. 69, p 877-892.

McGuire, R.K., and T.P. Barnhard (1981), "Effects of Temporal Variations in Seismicity on Seismic Hazard", Bull. Seis. Soc. Am., Vol. 71, p. 321-334.

McGuire, R. K. and K. M. Shedlock (1981), "Statistical Uncertainties in Seismic Hazard Evaluations in the United States," Bull. Seis. Soc. Am., Vol. 71, No. 4, p. 1287-1308.

Nuttli, O.W., and R.B. Herrmann (1978), "Credible Earthquakes for the Central United States:, Report 12, Misc. Paper S-73-1, U.S. Army Eng. Waterways Exp. Station (Vicksburg).

Nuttli, O.W., and R.B. Herrmann (1981), "Consequences of Earthquakes in the Mississippi Valley", Preprint 81-519, Amer. Soc. Civil Eng. Mtg, St. Louis, Oct.

Patwardhan, A., K. Sadigh, I.M. Idriss, and R. Youngs (1978), "Attenuation of Strong Ground Motion - Effect of Site Conditions, Transmission Path Characteristics, and Focal Depths", in preparation. See I.M. Idriss, "Characteristics of Earthquake Ground Motion", Proc., ASCE Specialty Conference of Earthquake Engineering and Soil Dynamics, Pasadena, June 1978.

Reagor, B.G., C.W. Stover, and S.T. Algermissen (1980), "Seismicity Map of the State of South Carolina", U.S.G.S., Misc. Field Map MF-1225.

Seeber, L. and S. Armbruster, (1981), "The 1886 Charleston, South Carolina Earthquake and the Appalachian Detachment", Jour. Geophys. Res., 86, B9, Sept. 10, p. 7874-7894.

Shannon and Wilson, Inc., and Agbabian Assoc. (1974), "Statistical analysis of Earthquake Ground Motion Parameters", USNRC, NUREG/CR-1175, Dec.

REFERENCES (Concluded)

TERA Corp. (1980), "Seismic Hazard Analysis-Solicitation of Expert Opinion", USNRC, NUREG/CR-1582, Aug.

Trifunac, M.D., (1976), "Preliminary Analysis of the Peaks of Strong Earthquake Ground Motion-Dependence of Peaks on Earthquake Magnitude, Epicentral Distance, and Recording Site Conditions", Bull. Seis. Soc. Am., Vol. 66, No. 1, Feb., p. 189-219.

Weichert, D.H. (1980), "Estimation of the Earthquake Recurrence Parameters for Unequal Observation Periods for Different Magnitudes", Bull. Seis. Soc. Am., Vol. 70, No. 4, p. 1337-1346.

Wentworth, C.M. and M. Mergner-Keefer, (1981), "Reverse Faulting along the Eastern Seaboard and the Potential for Large Earthquakes", in Earthquakes and Earthquake Engineering - Eastern United States, J.E. Beavers ed., Vol. 1, Ann Arbor Science Publishers, Inc., Ann Arbor, Michigan, p. 109-128.

Weston Geophysical Corp. (1982), "Estimation of Seismicity Parameters for New England", Rept. Prepared for Yankee Atomic Electric Co., April.

Yankee Atomic Electric Company (1982), "Supplemental Seismic Probabilistic Study," Report YAEC-1331.

TABLE 1
GENERAL ASSUMPTIONS USED IN SEISMIC HAZARD ANALYSIS

1.	Earthquake locations represented by seismogenic zones with a homogeneous location distribution.	1.	In general, realistic. Conservative for sites located away from active fault zones, unconservative for sites located near active fault zones.
2.	Earthquake magnitudes can be estimated for intensities.	2.	Realistic
3.	Truncated exponential distribution represents earchquake sizes.	3.	Realistic
4.	$m_{b,max}$ represents largest earthquakes.	4.	In general, realistic. Conservative for zones with lower $m_{b,max}$; unconservative for zones with higher $m_{b,max}$.
5.	Rate of activity represented by historical rate of occurrence.	5.	Realistic
6.	Peak acceleration estimated by attenuation function as $f(m_b, \Delta)$.	6.	Realistic
7.	Uncertainty in peak acceleration represented by lognormal distribution with $\sigma_{\ln a} = 0.6$.	7.	Realistic

TABLE 2

SEISMOGENIC ZONES AND ASSOCIATED SEISMICITY PARAMETERS

Zone Hypothesis	Dominant Zone(s)*	Area (10^4 km^2)	$m_{b,max}$	Nuttli-Herrmann Conversion		Weston Conversion	
				Activity Rate**	Richter b-value	Activity Rate**	Richter b-value
Geologic Provinces	Central New England	10.34	5.5/6.0/6.5	0.0443	1.39/1.21/1.03	0.0262	1.13/0.98/0.83
Tectonic Provinces	Northern Piedmont	30.74	5.8/6.3/6.8	0.1244	1.25/1.09/0.93	0.0622	1.25/1.08/0.92
U.S. Geological Survey	103	6.33	5.3/5.8/6.3	0.0712	1.20/1.04/0.88	0.0441	1.18/1.03/0.88
	107	3.35	5.8/6.3/6.8	0.0205	1.30/1.13/0.96	0.0100	1.13/0.98/0.83
Northern Appalachian	Northern Appalachian	39.37	5.8/6.3/6.8	0.1376	1.25/1.08/0.92	0.0758	1.18/1.03/0.88
Decollement, Version 1	Background	9.41	6.3	0.0341	1.02	0.0300	1.03
Decollement, Version 2	Decollement	70.78	7.0	0.2312	1.16	0.2312***	1.16***
Mesozoic Rift, Version 1	Connecticut Valley Rift	7.09	6.0/7.0	0.0350	1.14/1.14	0.0186	0.87/0.87
Mesozoic Rift, Version 2	Connecticut Valley Rift	7.39	6.0/7.0	0.0350	1.14/1.14	0.0186	0.87/0.87
Mesozoic Intersection, Version 1	Connecticut Intersection	0.45	6.0/7.0	0.0056	1.42/1.42	0.0038	0.95/0.95
	Background	5.73	5.8	0.0319	1.36	0.0101	1.32
Mesozoic Intersection, Version 2	Connecticut Intersection	0.92	6.0/7.0	0.0056	1.42/1.42	0.0033	1.01/1.01
	Background	5.67	5.8	0.0319	1.36	0.0101	1.32
Mafic Plutons	Background	7.33	5.8	0.0319	1.36	0.0101	1.32

*Zone(s) which dominate(s) seismic hazard at Millstone

**For $m_b \geq 4.5$

***Values from Nuttli-Herrmann conversion used instead of those from Weston conversion because the zone extends into the southeastern U.S.

TABLE 3
UNCERTAINTIES REPORTED FOR ATTENUATION EQUATIONS

REFERENCE	DATA BASE	$\sigma_{\ln a}$
Campbell (1981b)	Western U.S.	0.37
Cornell et al. (1979)	Western U.S.	0.57
Donovan (1973)	World-wide	0.84
Donovan (1974)	San Fernando	0.481
Donovan (1974)	World-wide	0.707
Esteva & Villaverde (1974)	Western U.S.	0.64
Joyner and Boore (1981)	Western U.S.	0.60
McGuire (1974)	Western U.S.	0.51
McGuire (1978a)	Western U.S.	0.62
Patwardhan et al. (1978)	California, Japan, Nicaragua, India (Shallow focus)	0.58
Shannon and Wilson, Inc., and Agbabian Assoc. (1979)	Western U.S.	0.573
Trifunac (1976)	Western U.S.	0.60*

* Calculated using procedure discussed in McGuire (1978b).

TABLE 4

BOUNDS ON EFFECTIVE PEAK ACCELERATION

MM Intensity	Corresponding Value of m_b, max (Equation 1****)	Corresponding Value of m_b,max (Equation 2****)	Upper Bound Sustained Acceleration	Upper Bound Peak Acceleration (g)***
VI	4.8	4.5	0.20*	0.25
VI-VII	5.0	4.8	0.25**	0.30
VII	5.3	5.1	0.30*	0.37
VII-VIII	5.5	5.5	0.40**	0.50
VIII	5.8	5.8	0.50*	0.62
VIII-IX	6.0	6.1	0.65**	0.80
IX	6.3	6.5	0.80*	1.00

* From R. P. Kennedy, Personal Communication, 1981

** Obtained by interpolation

*** Calculated as 1.25 times the Upper Bound Sustained Acceleration (see text)

**** See Section 4.1

TABLE 5

ANNUAL FREQUENCIES OF EXCEEDANCE

Aggregate Curve	Probability	Peak Acceleration (cm/sec^2) 100	200	300	400	500	600	700	800	900	980
1	0.004	$.48 \times 10^{-3}$	$.64 \times 10^{-4}$	$.14 \times 10^{-4}$	$.34 \times 10^{-5}$	$.83 \times 10^{-6}$	$.21 \times 10^{-6}$	$.78 \times 10^{-7}$	$.33 \times 10^{-7}$	$.12 \times 10^{-7}$	$.59 \times 10^{-8}$
2	0.163	$.29 \times 10^{-3}$	$.60 \times 10^{-4}$	$.21 \times 10^{-4}$	$.95 \times 10^{-5}$	$.47 \times 10^{-5}$	$.25 \times 10^{-5}$	$.14 \times 10^{-5}$	$.84 \times 10^{-6}$	$.53 \times 10^{-6}$	$.38 \times 10^{-6}$
3	0.127	$.11 \times 10^{-2}$	$.23 \times 10^{-3}$	$.84 \times 10^{-4}$	$.37 \times 10^{-4}$	$.19 \times 10^{-4}$	$.10 \times 10^{-4}$	$.57 \times 10^{-5}$	$.33 \times 10^{-5}$	$.21 \times 10^{-5}$	$.15 \times 10^{-5}$
4	0.084	$.58 \times 10^{-3}$	$.14 \times 10^{-3}$	$.53 \times 10^{-4}$	$.25 \times 10^{-4}$	$.13 \times 10^{-4}$	$.69 \times 10^{-5}$	$.39 \times 10^{-5}$	$.23 \times 10^{-5}$	$.15 \times 10^{-5}$	$.11 \times 10^{-5}$
5	0.129	$.14 \times 10^{-3}$	$.21 \times 10^{-4}$	$.57 \times 10^{-5}$	$.19 \times 10^{-5}$	$.63 \times 10^{-6}$	$.20 \times 10^{-6}$	$.58 \times 10^{-7}$	0	0	0
6	0.074	$.85 \times 10^{-3}$	$.14 \times 10^{-3}$	$.37 \times 10^{-4}$	$.12 \times 10^{-4}$	$.41 \times 10^{-5}$	$.15 \times 10^{-5}$	$.55 \times 10^{-6}$	0	0	0
7	0.074	$.36 \times 10^{-3}$	$.64 \times 10^{-4}$	$.19 \times 10^{-4}$	$.62 \times 10^{-5}$	$.21 \times 10^{-5}$	$.71 \times 10^{-6}$	$.21 \times 10^{-6}$	0	0	0
8	0.168	$.10 \times 10^{-3}$	$.13 \times 10^{-4}$	$.30 \times 10^{-5}$	$.71 \times 10^{-6}$	$.15 \times 10^{-6}$	0	0	0	0	0
9	0.082	$.59 \times 10^{-3}$	$.66 \times 10^{-4}$	$.11 \times 10^{-4}$	$.19 \times 10^{-5}$	$.34 \times 10^{-6}$	0	0	0	0	0
10	0.095	$.33 \times 10^{-3}$	$.49 \times 10^{-4}$	$.11 \times 10^{-4}$	$.27 \times 10^{-5}$	$.62 \times 10^{-6}$	0	0	0	0	0

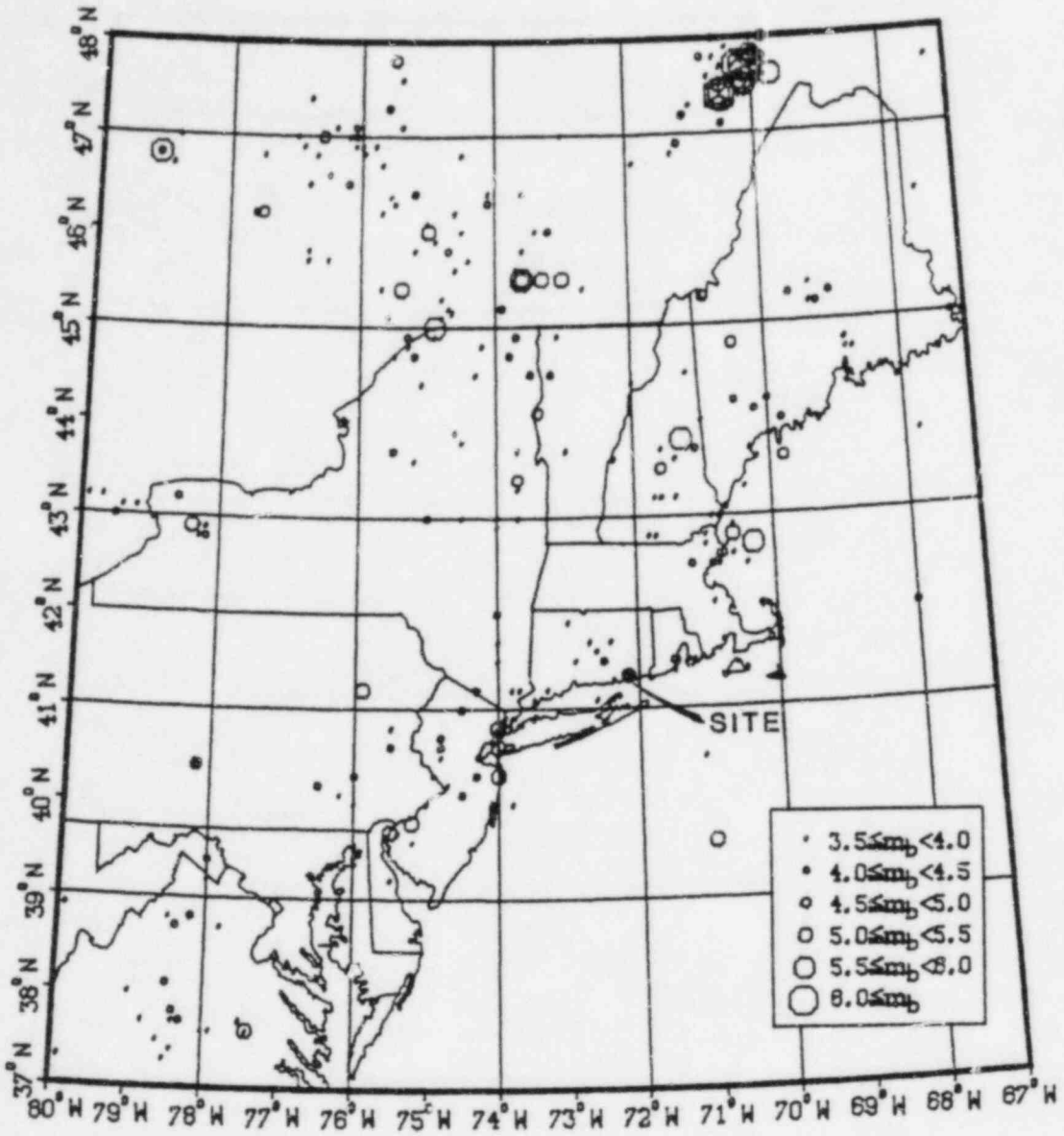

Figure 1

Seismicity in the Vicinity of the Site

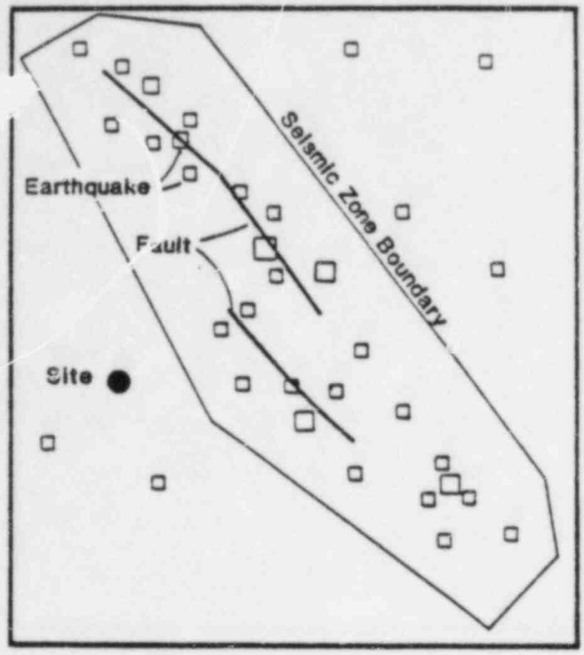

(A)

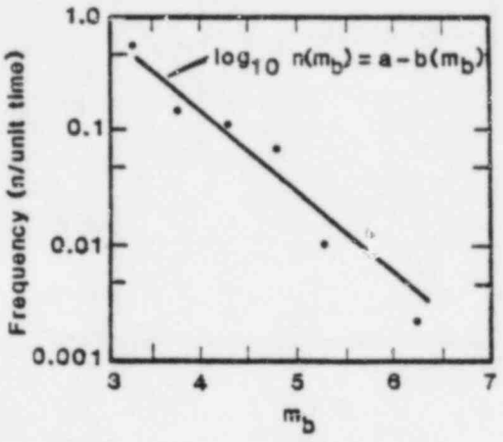

(B)

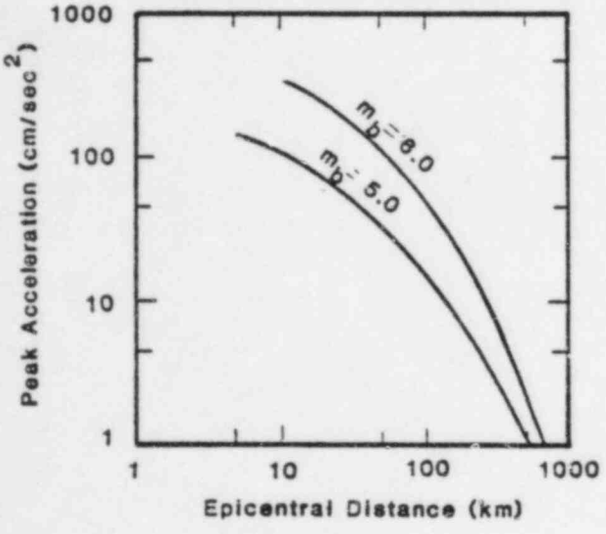

(C)

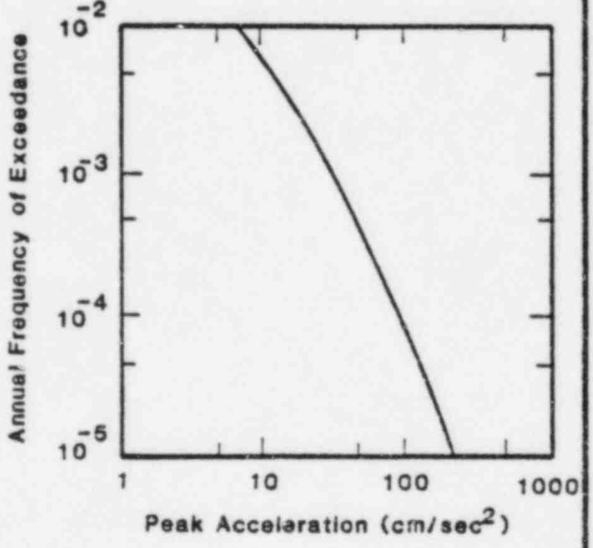

(D)

Figure 2

Conceptual Representation of Steps Involved in Seismic Hazard Evaluation

Dames & Moore

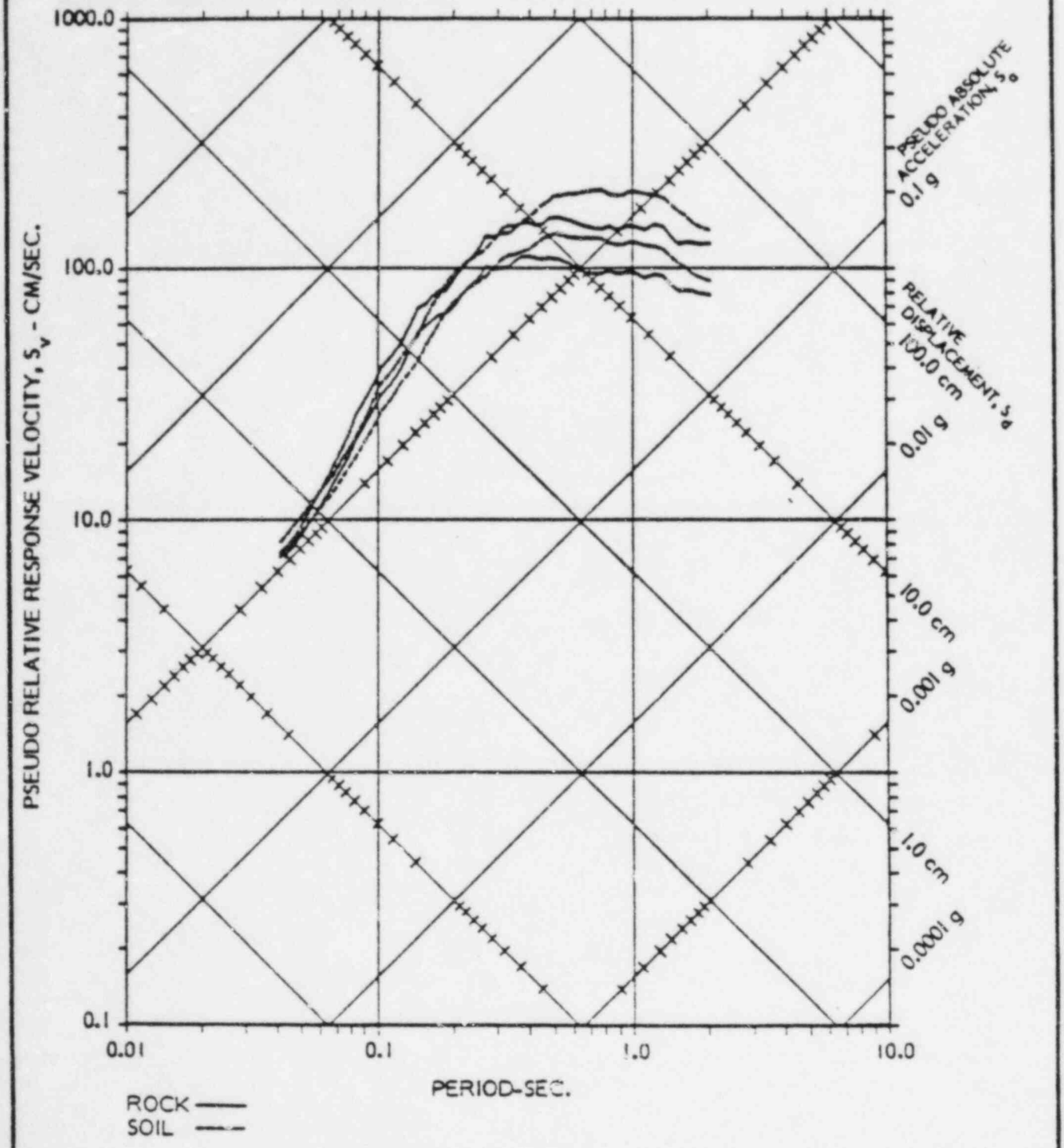

Figure 3

Mean and Mean + σ Spectra for Near-Source Magnitude 5.8 Earthquakes (from Bernreuter, 1981)

Dames & Moore

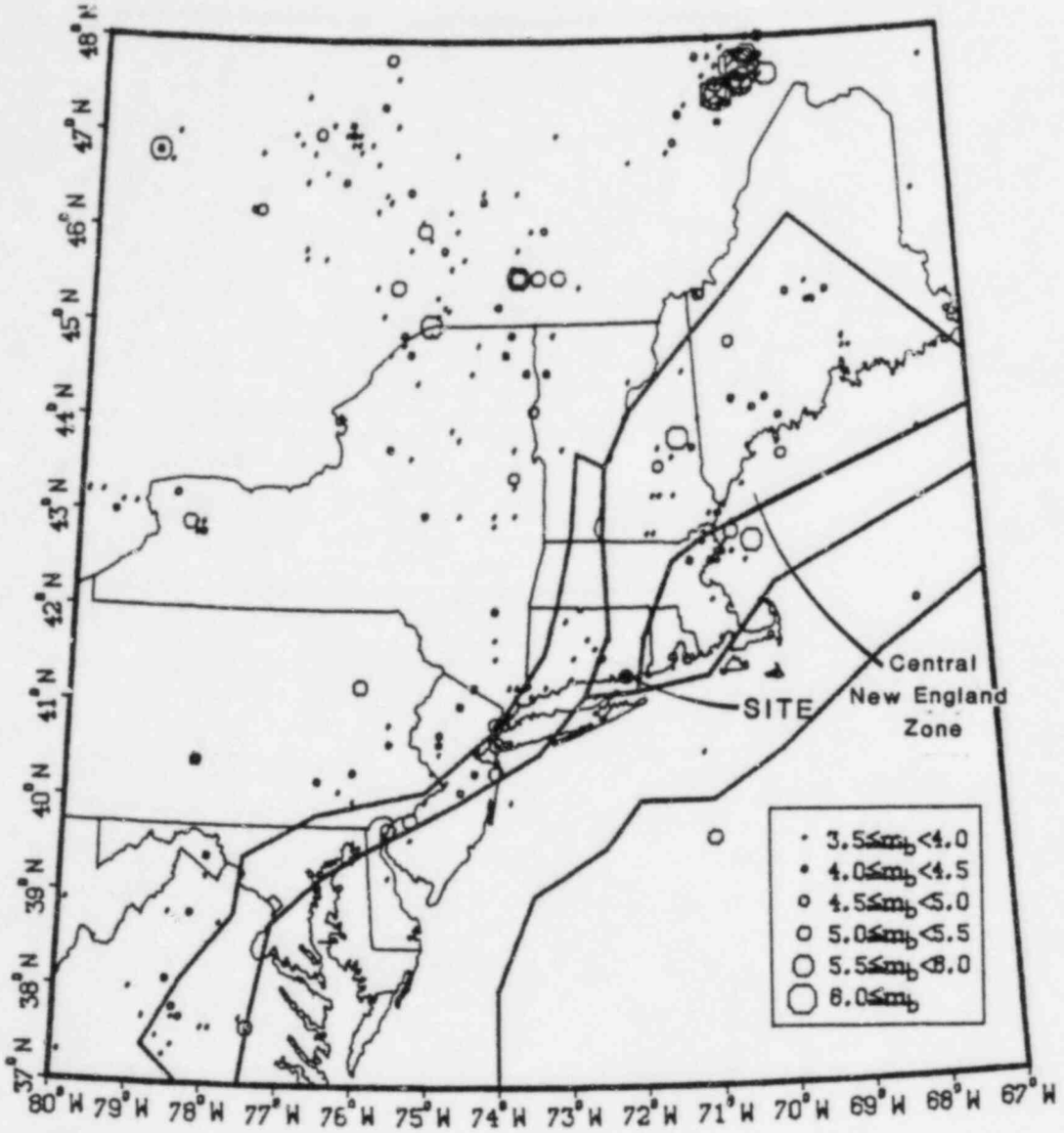

Figure 4

Geologic Province Zones

Dames & Moore

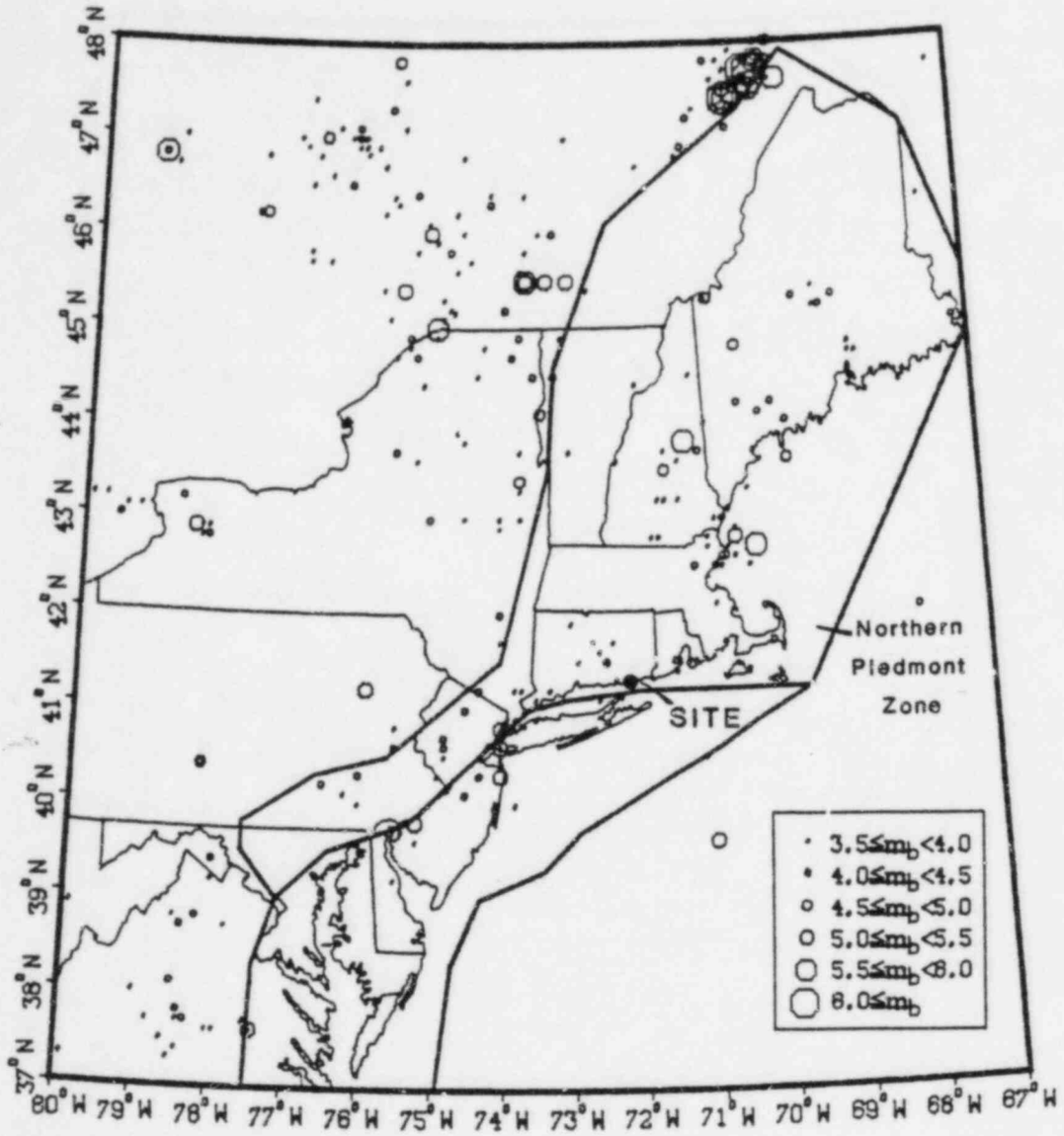

Figure 5

Tectonic Province Zones

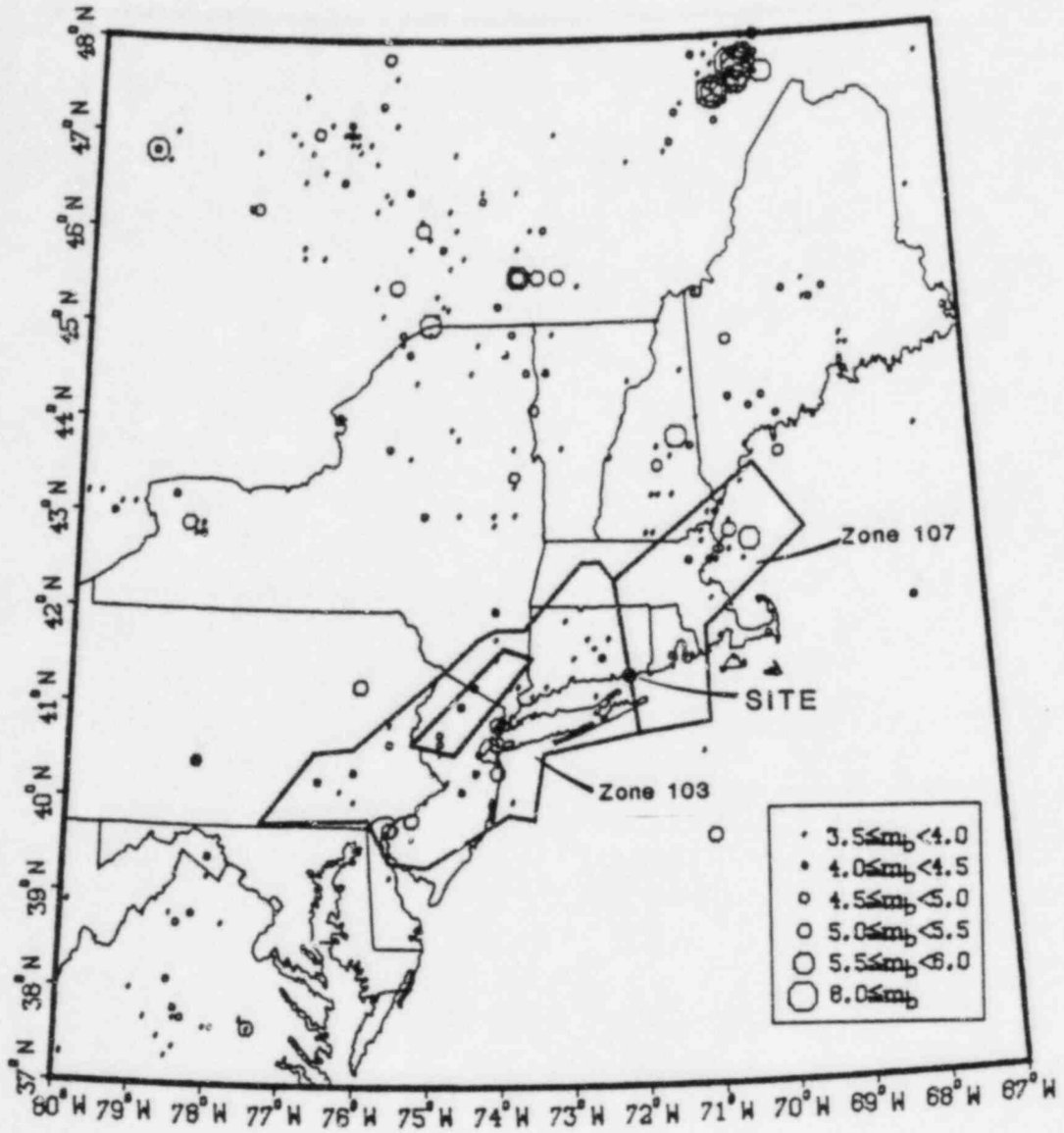

Figure 6

U.S. Geological Survey Zones

Dames & Moore

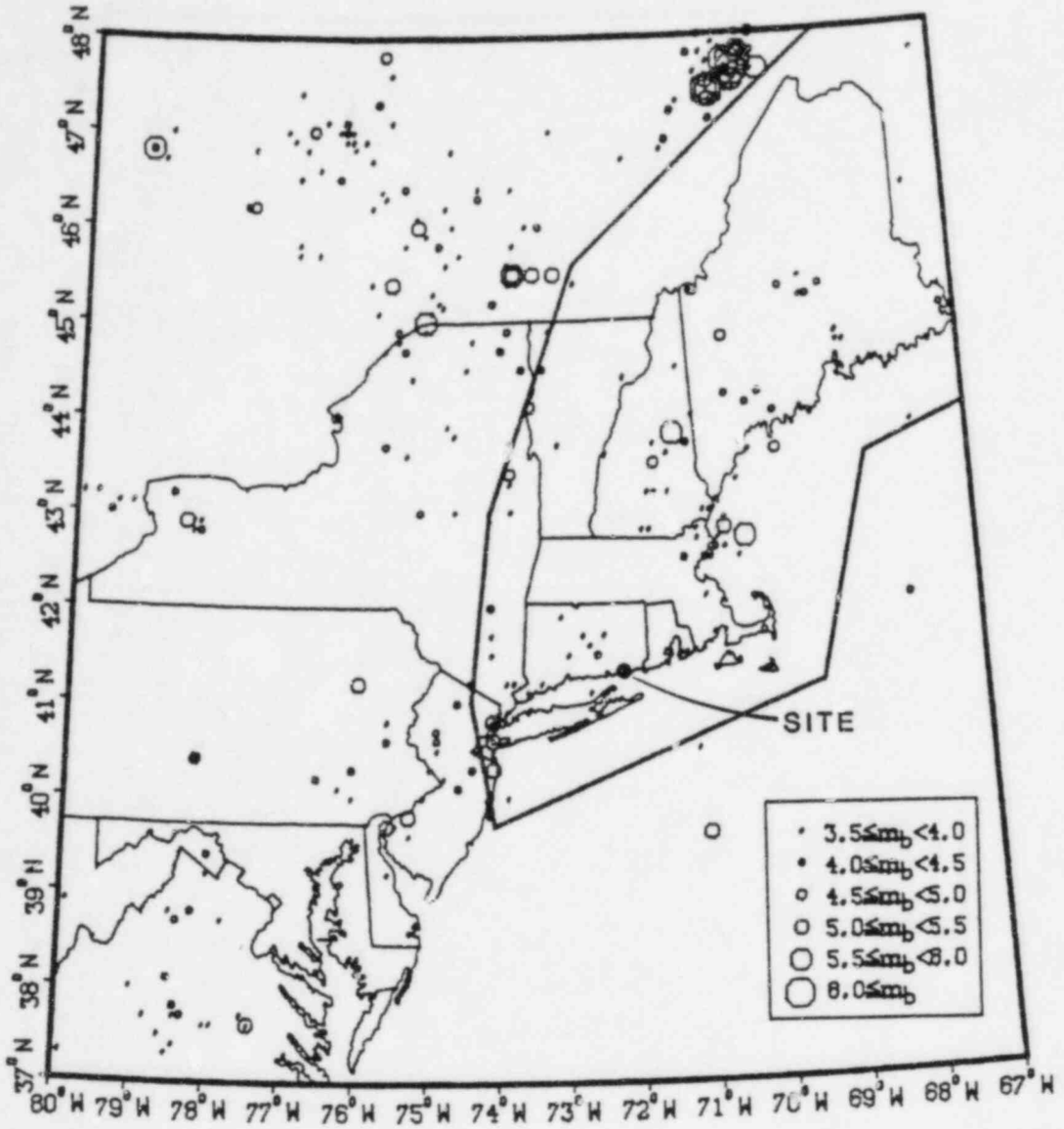

Figure 7
Northern Appalachian Zone

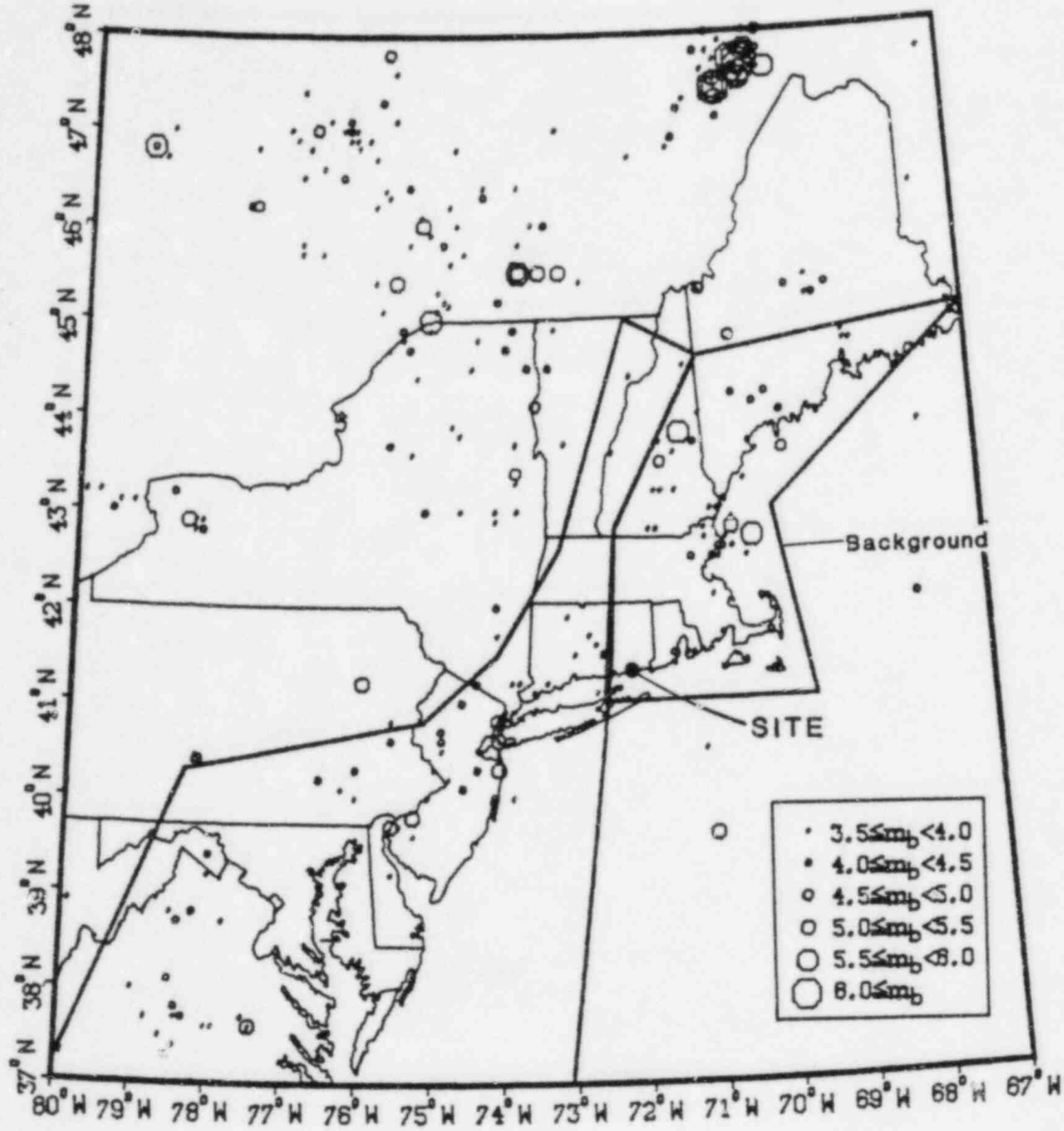

Figure 8

Decollement Zone, Version 1

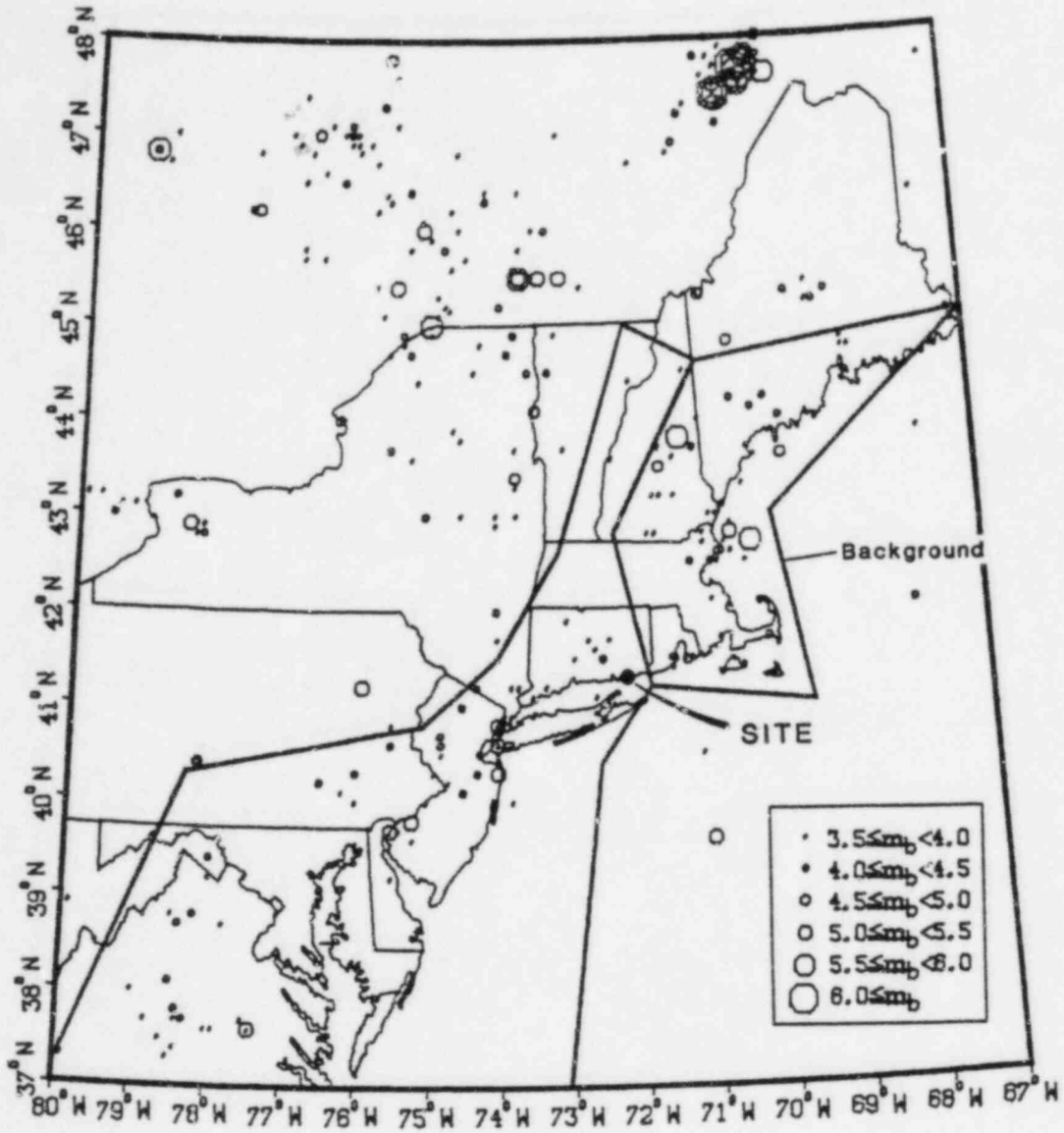

Figure 9
Decollement Zone, Version 2

Dames & Moore

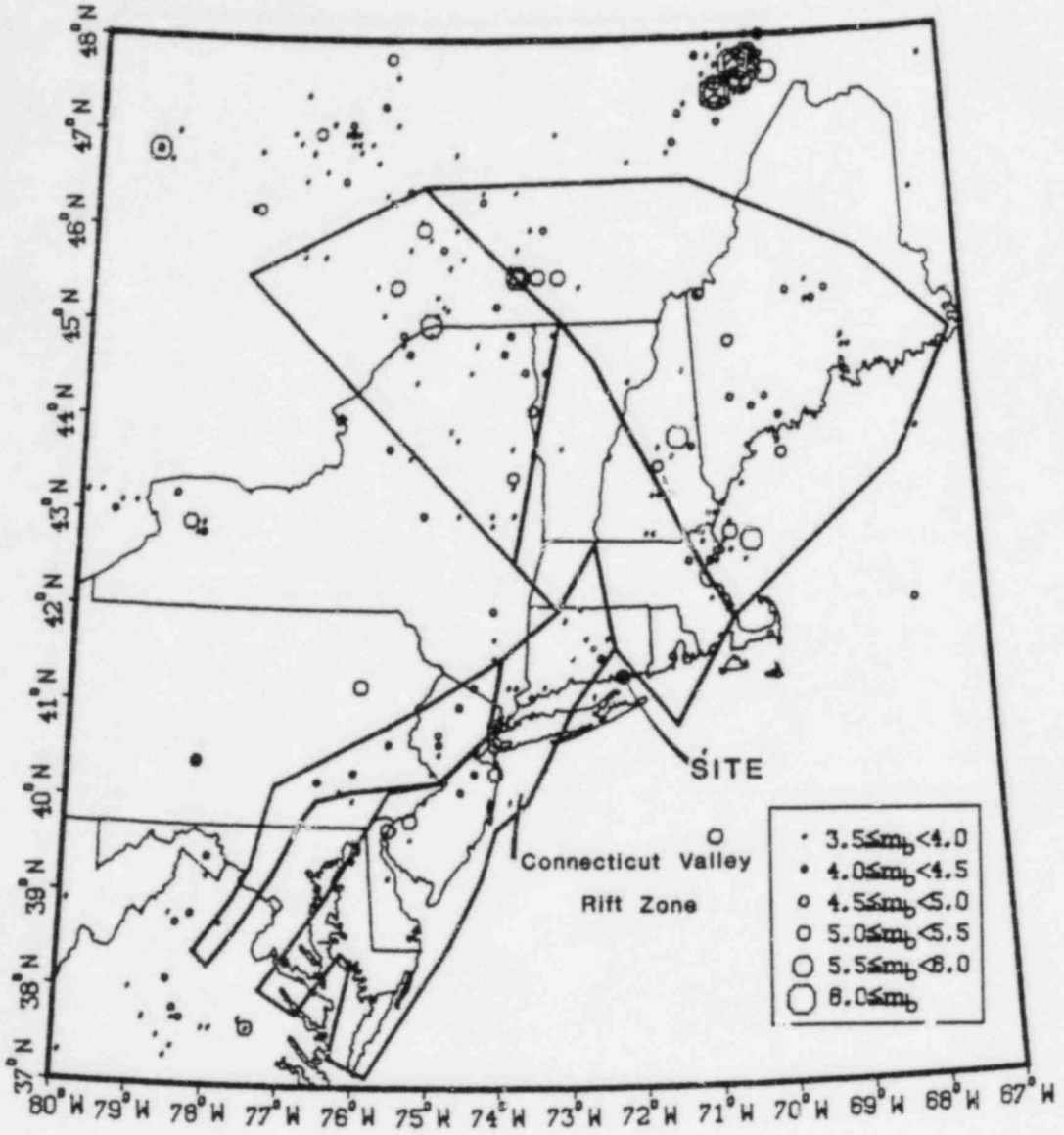

Figure 10

Mesozoic Rift Zones, Version 1

Dames & Moore

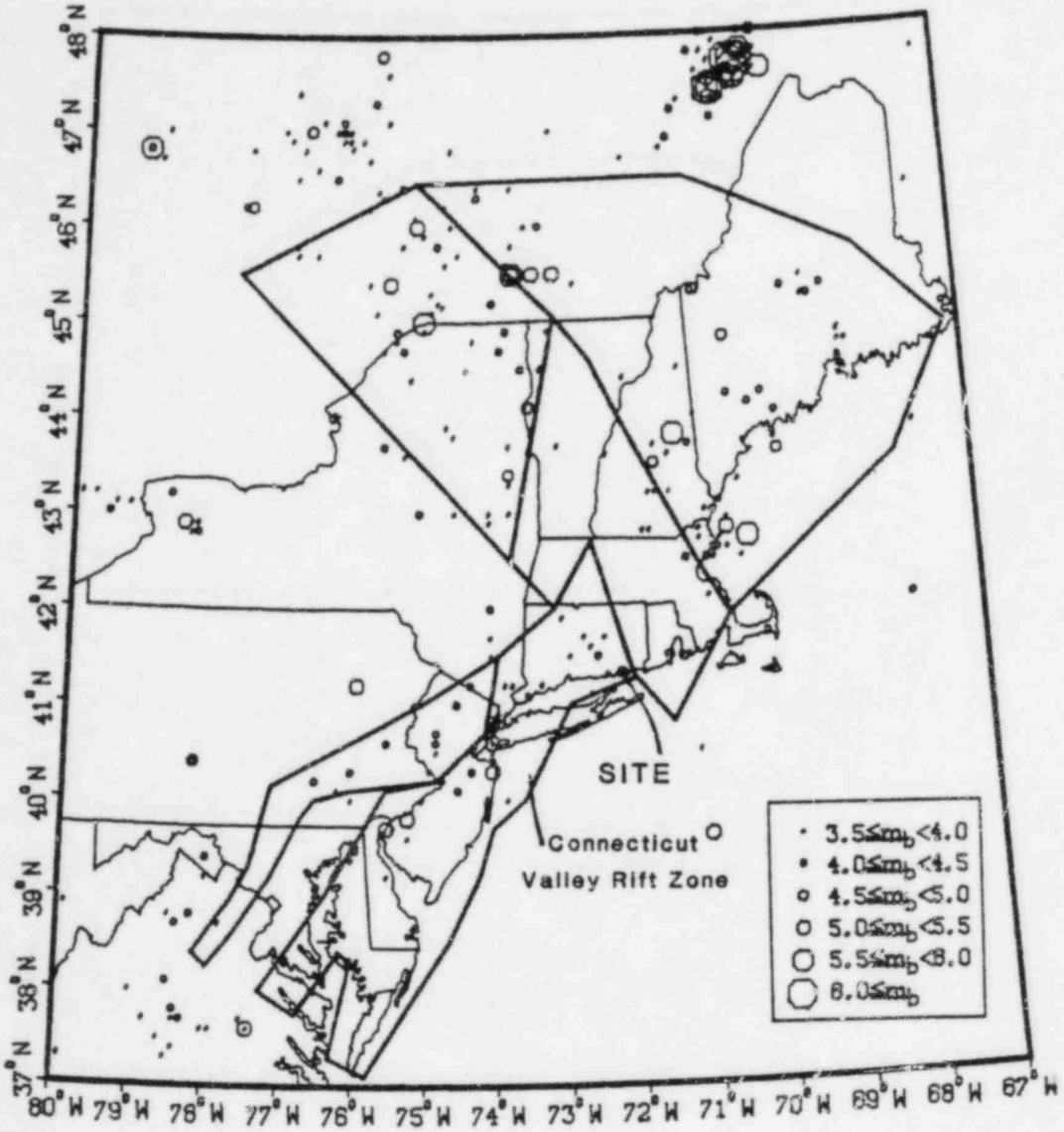

Figure 11

Mesozoic Rift Zones, Version 2

Dames & Moore

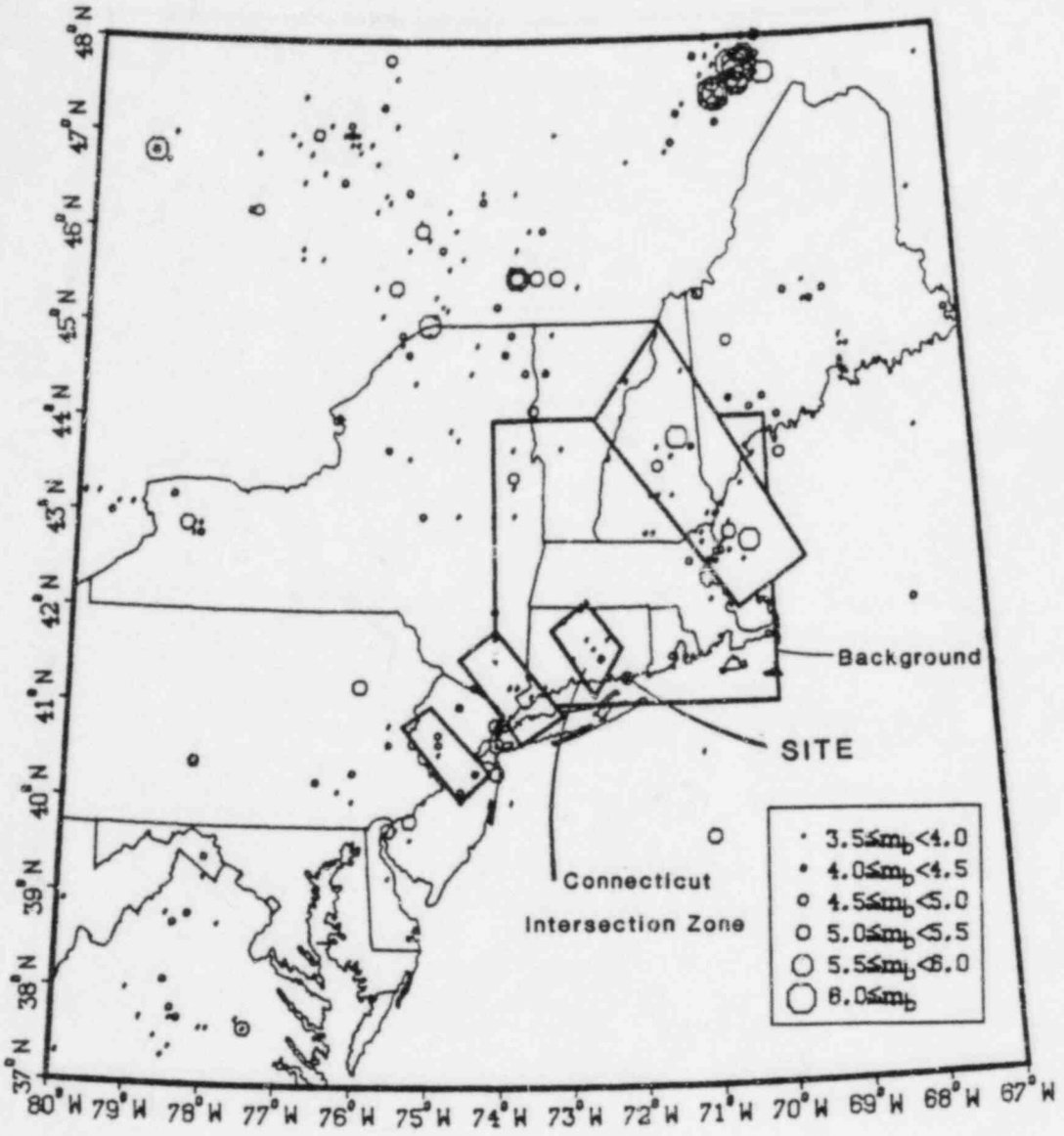

Figure 12

Mesozoic Intersection Zones, Version 1

Dames & Moore

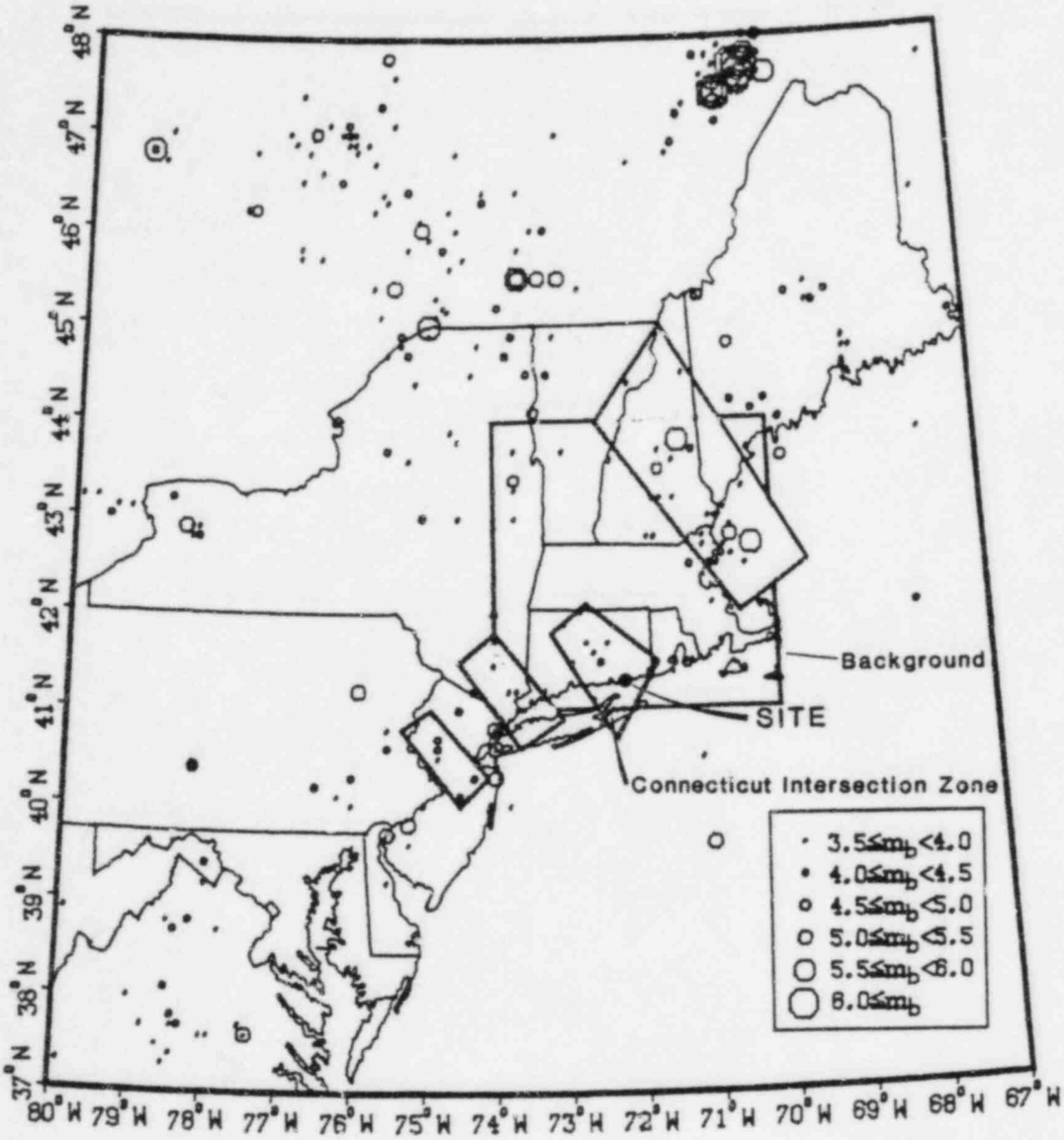

Figure 13

Mesozoic Intersection Zones, Version 2

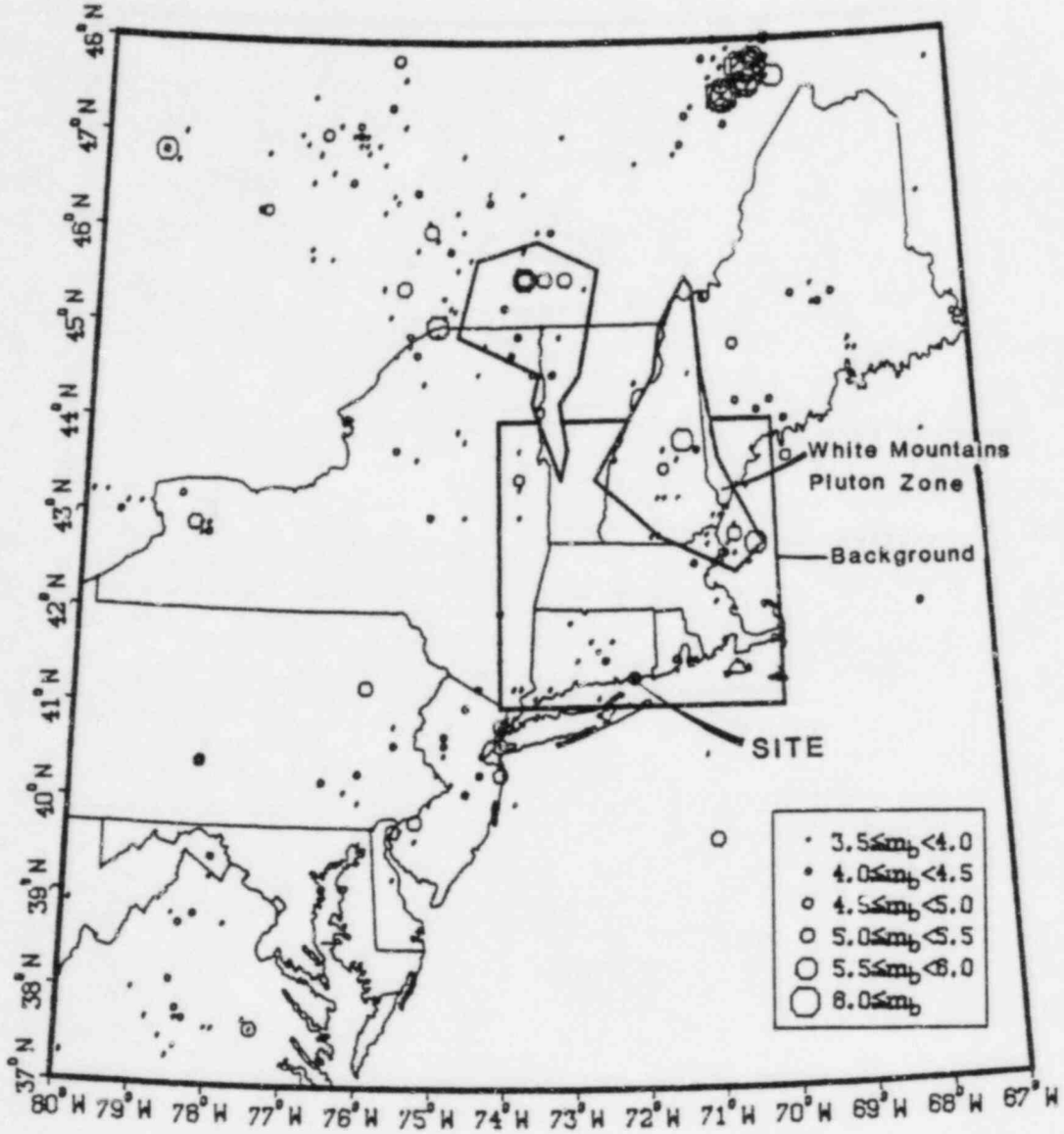

Figure 14

Mafic Pluton Zones

Dames & Moore

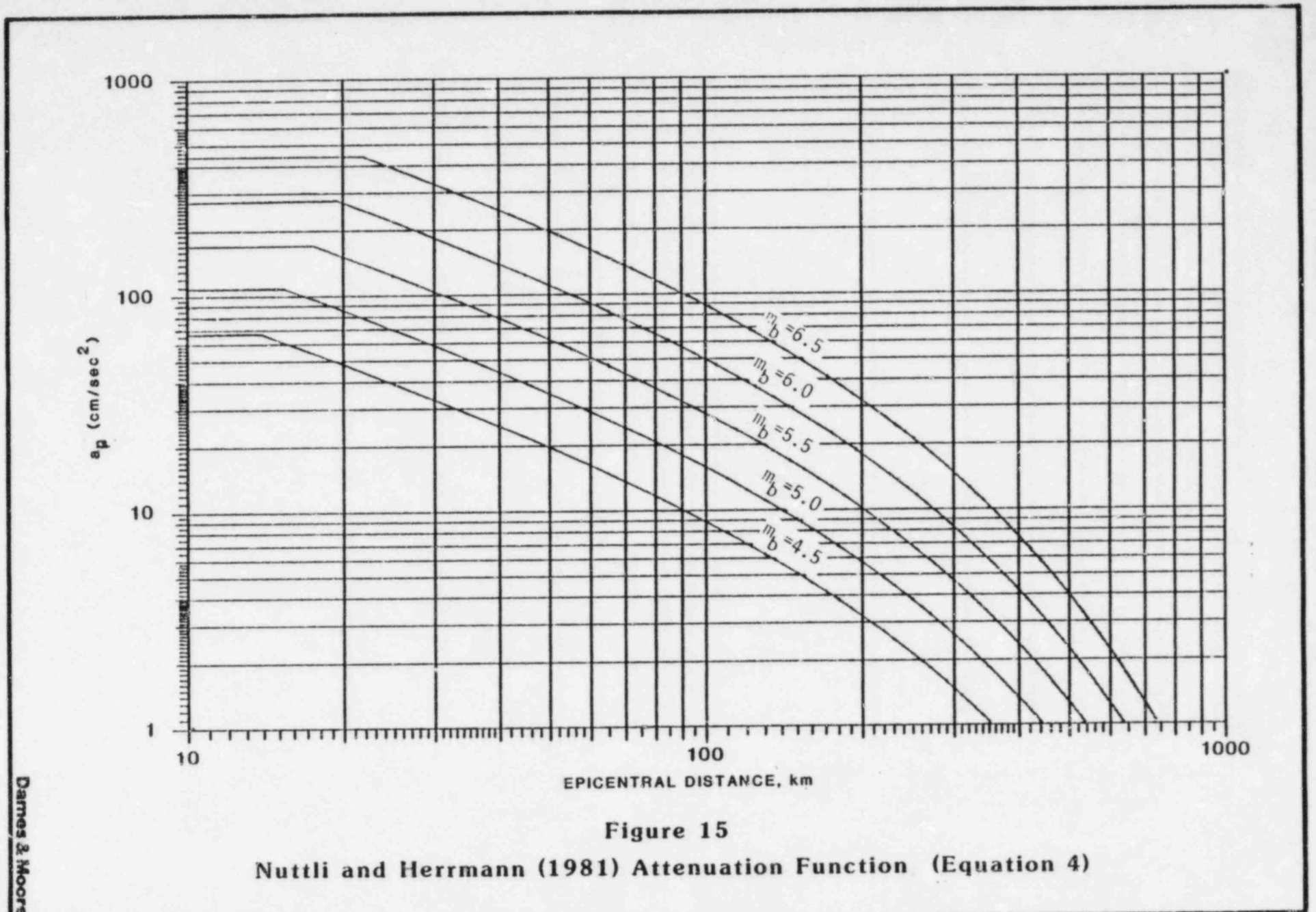

Figure 15

Nuttli and Herrmann (1981) Attenuation Function (Equation 4)

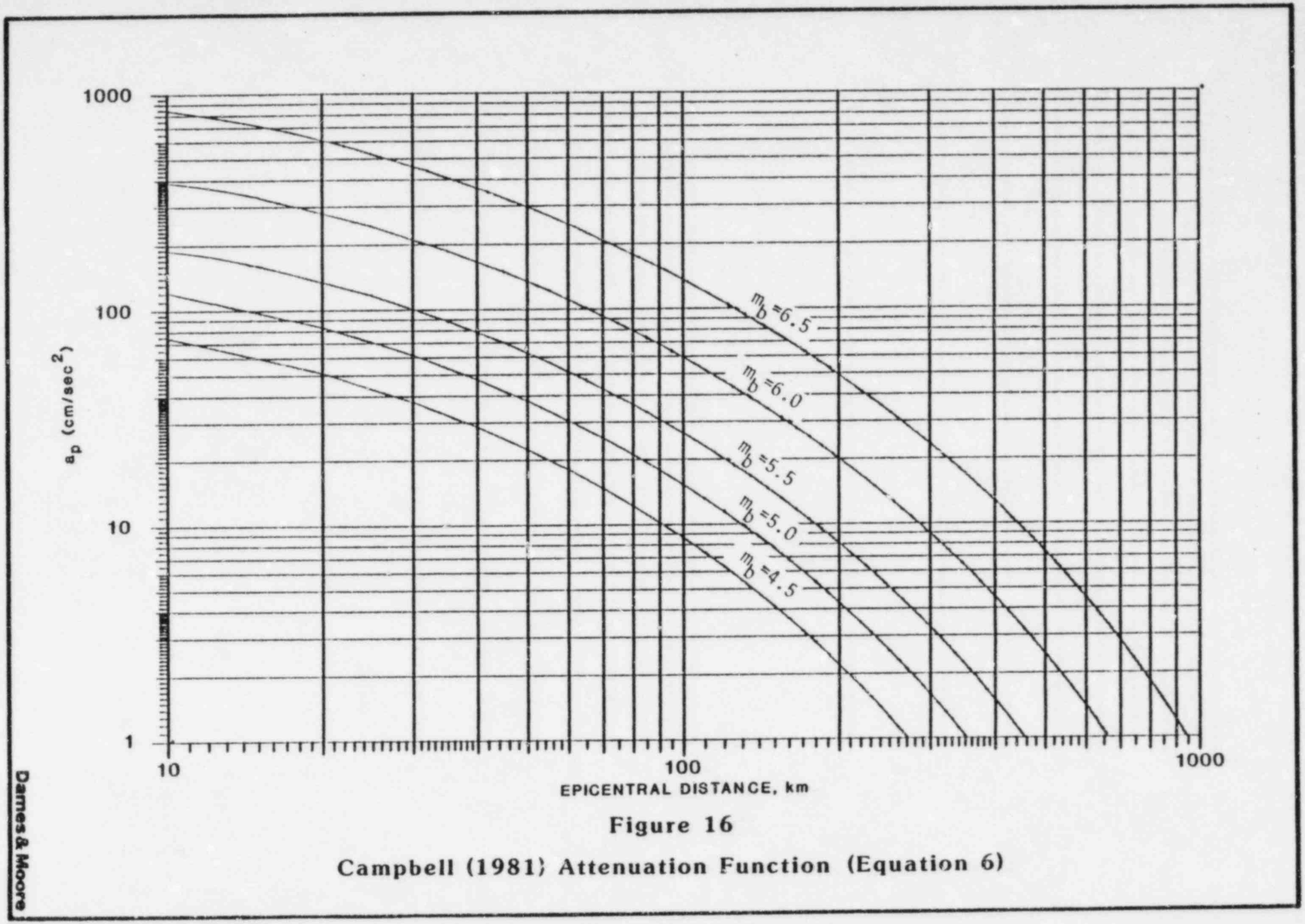

Figure 16

Campbell (1981) Attenuation Function (Equation 6)

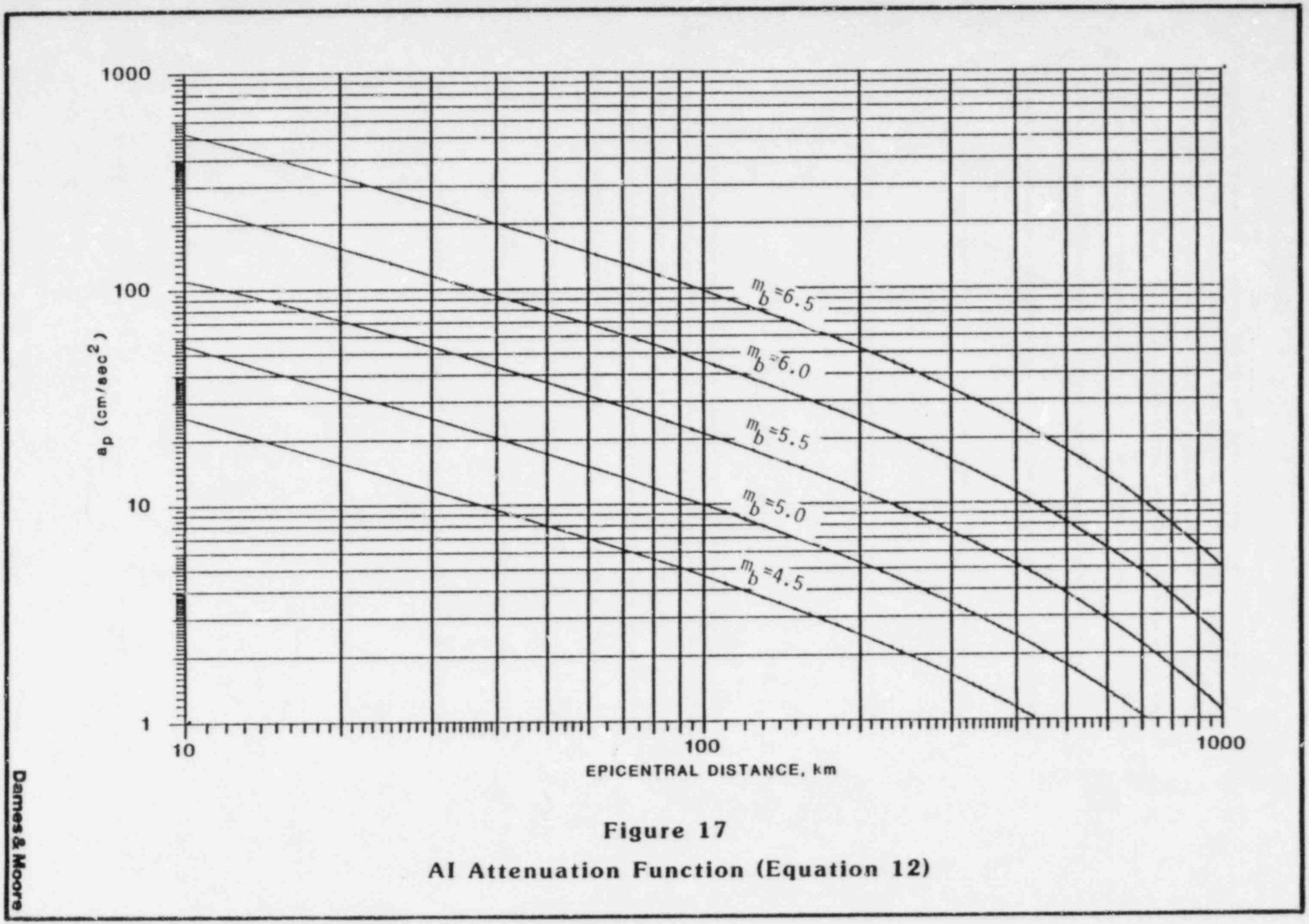

Figure 17

AI Attenuation Function (Equation 12)

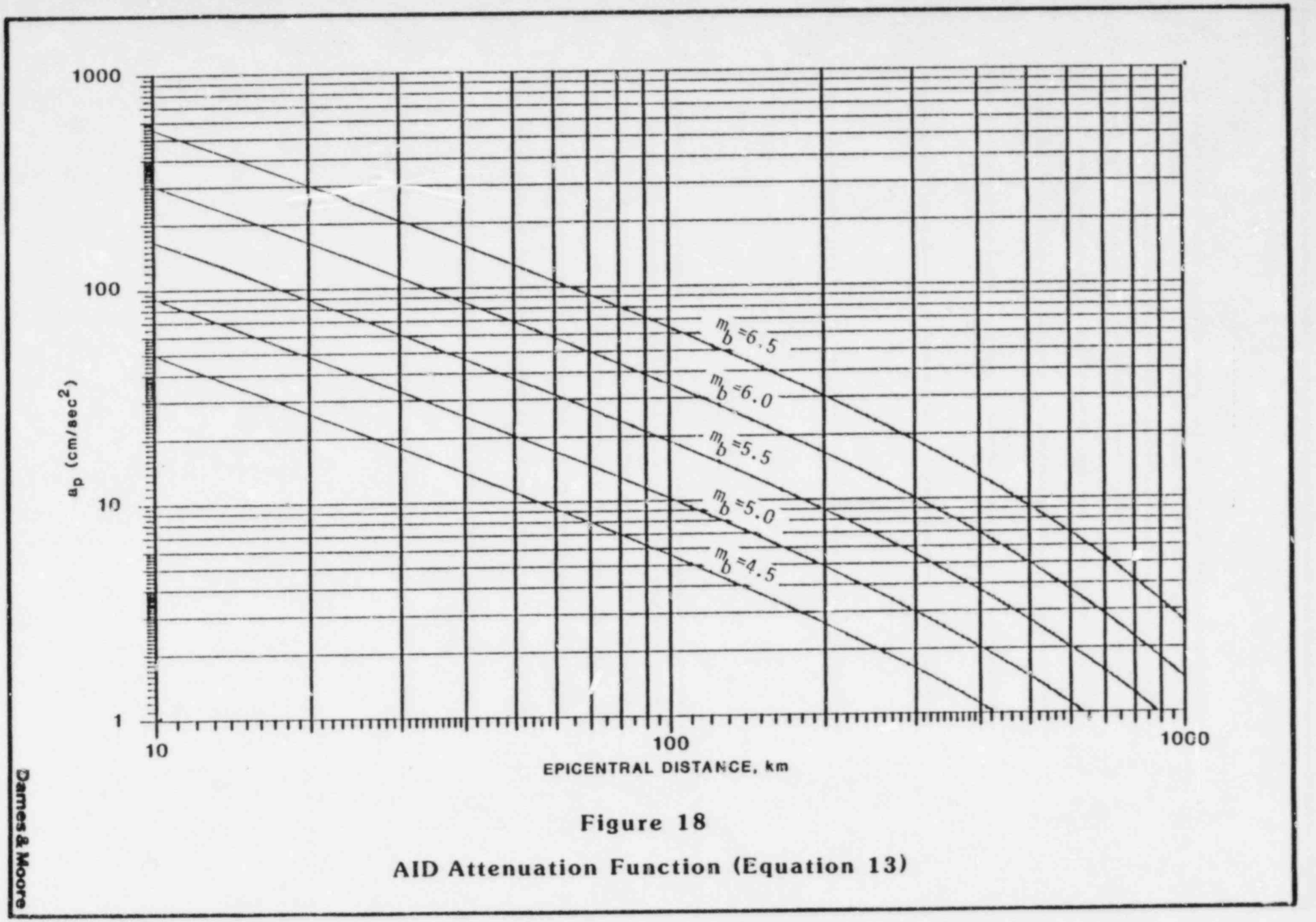

Figure 18

AID Attenuation Function (Equation 13)

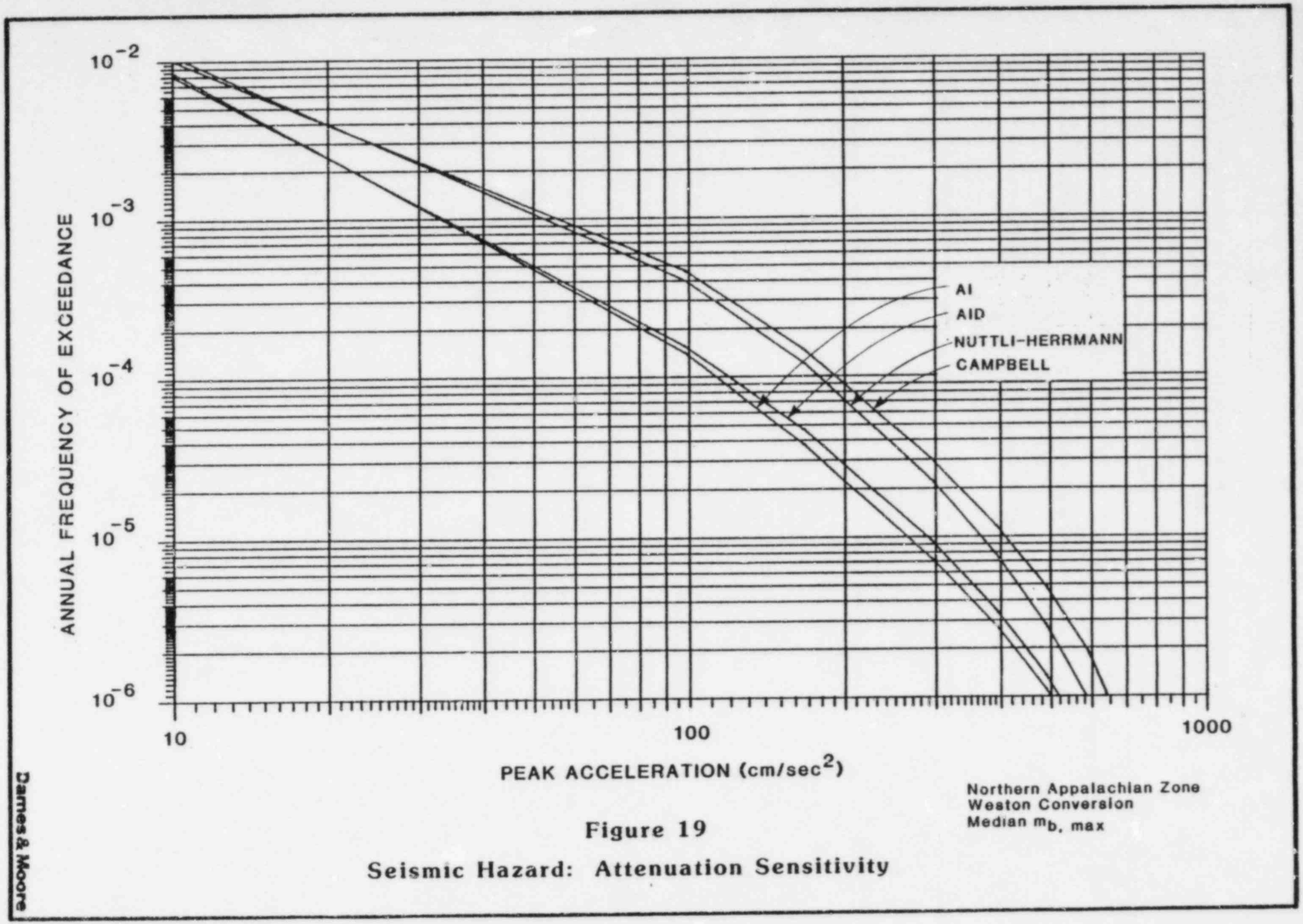

Figure 19

Seismic Hazard: Attenuation Sensitivity

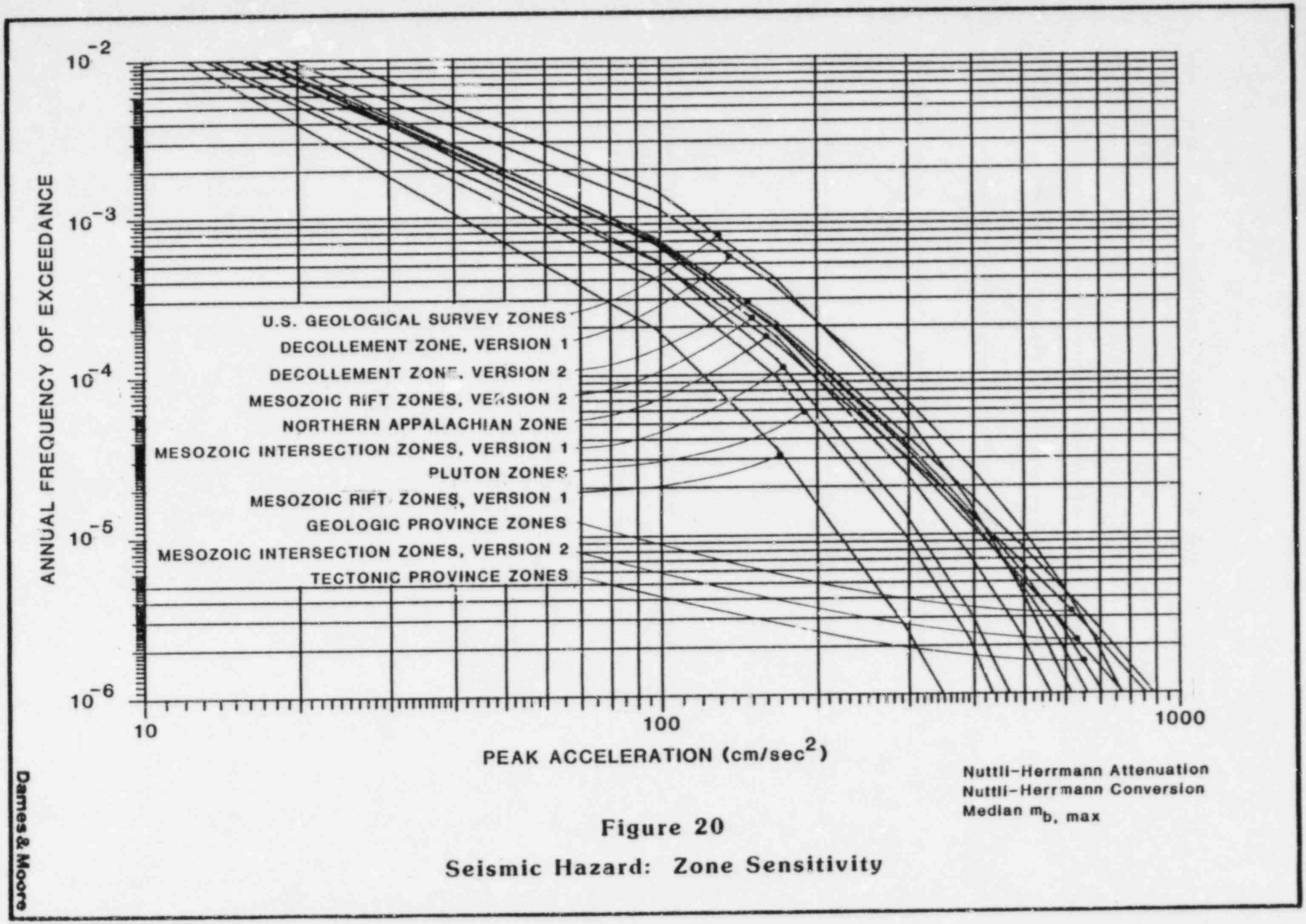

Figure 20

Seismic Hazard: Zone Sensitivity

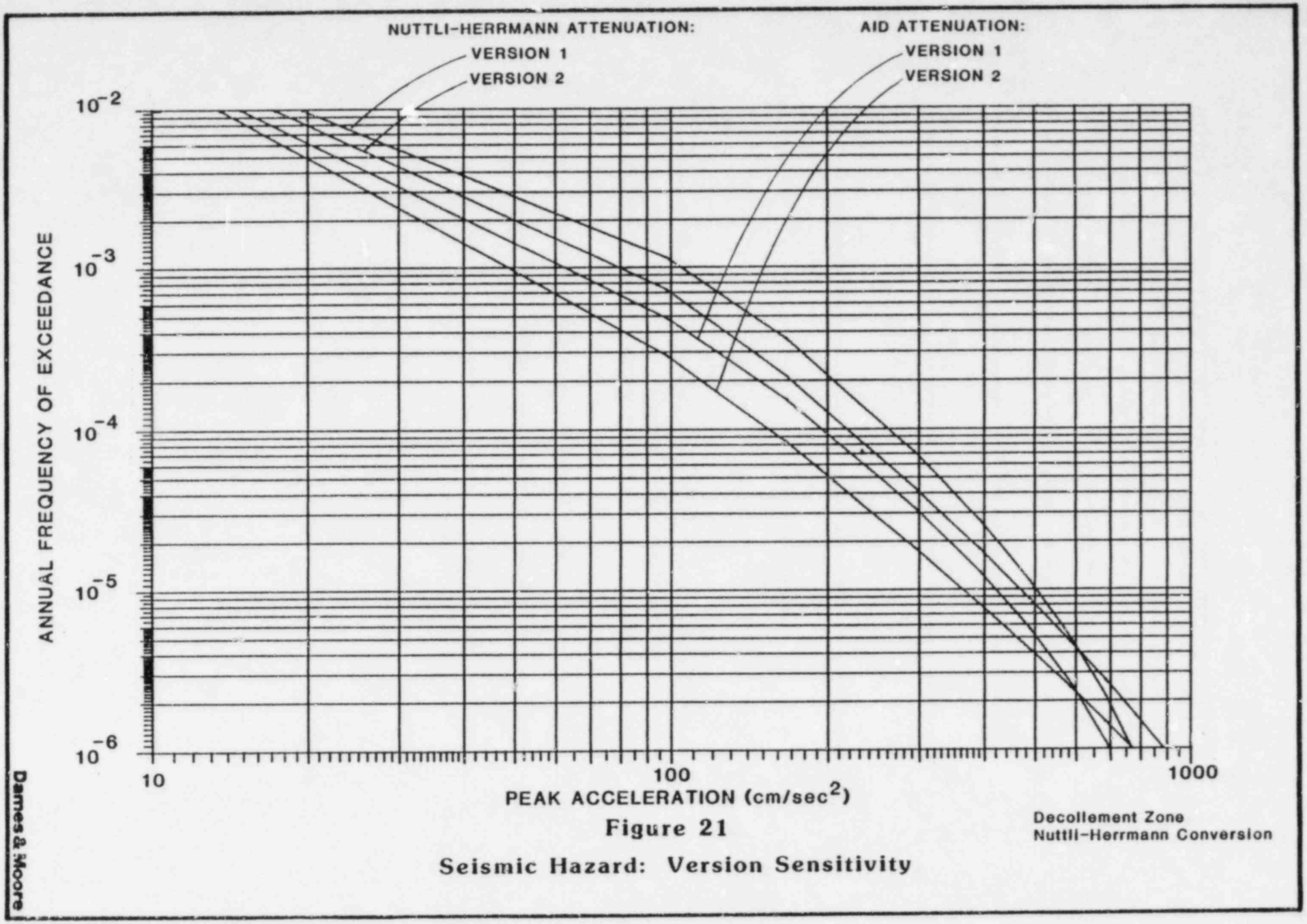

Figure 21

Seismic Hazard: Version Sensitivity

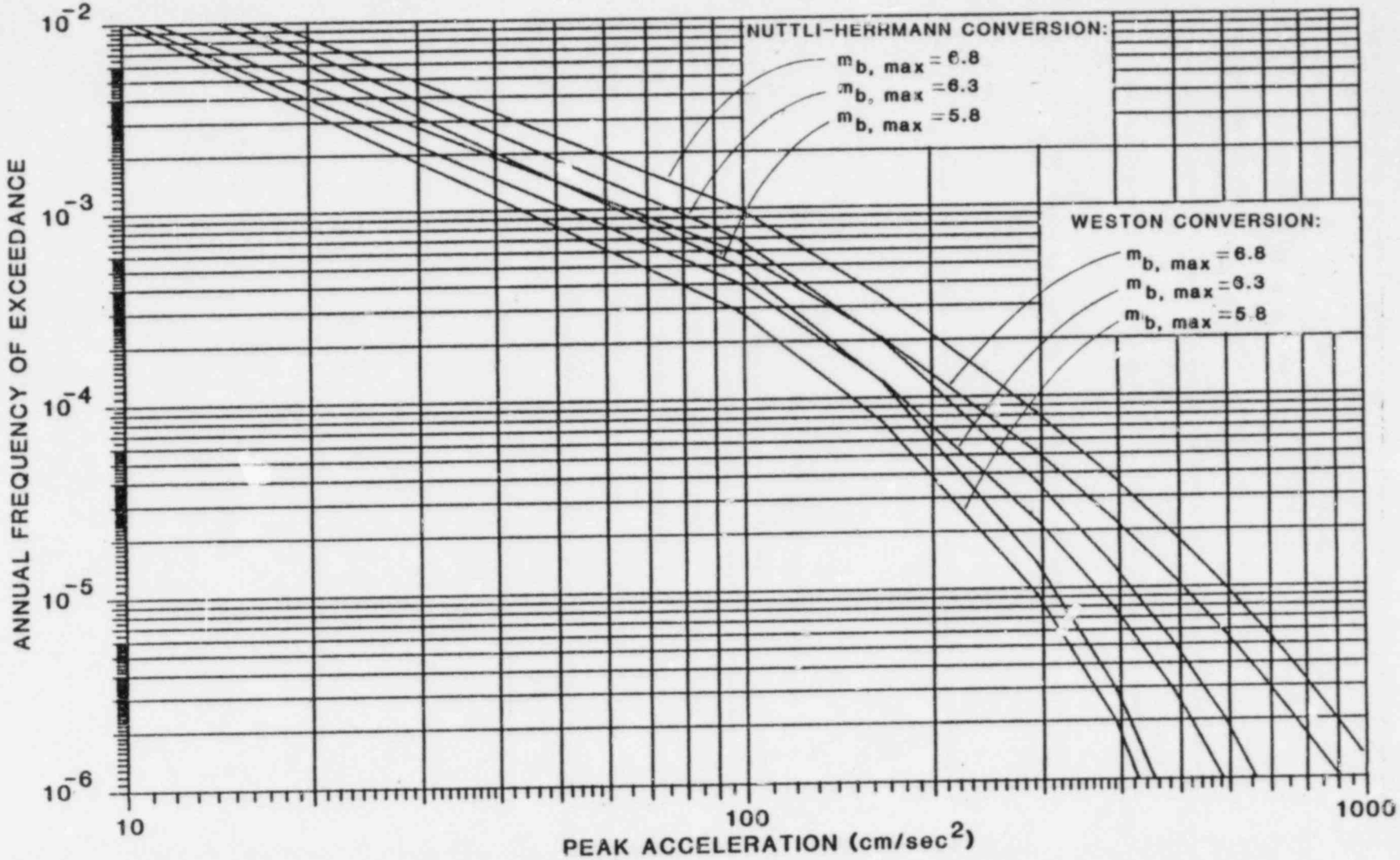

Figure 22

Seismic Hazard: $m_{b,\,max}$ Sensitivity

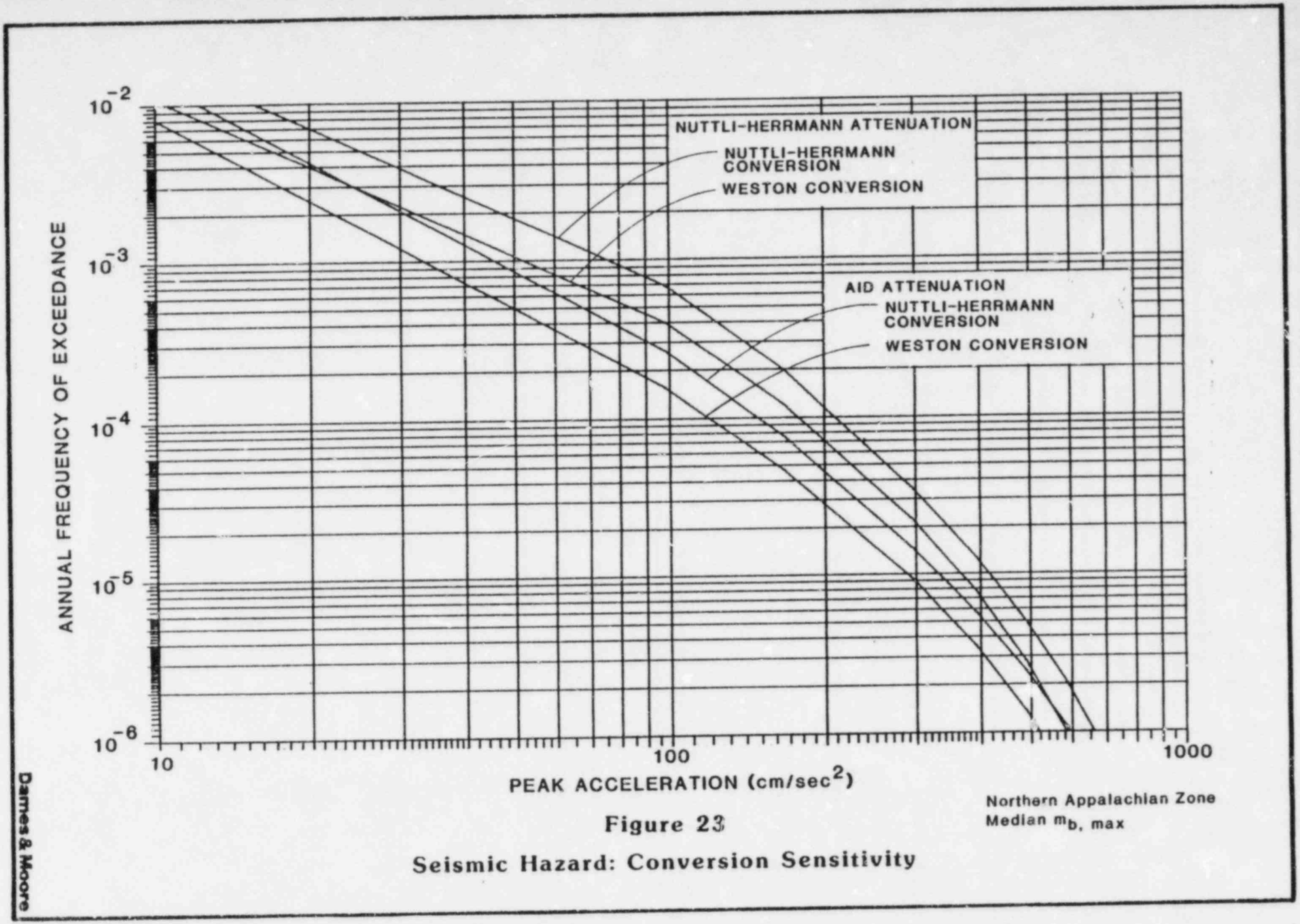

Figure 23

Seismic Hazard: Conversion Sensitivity

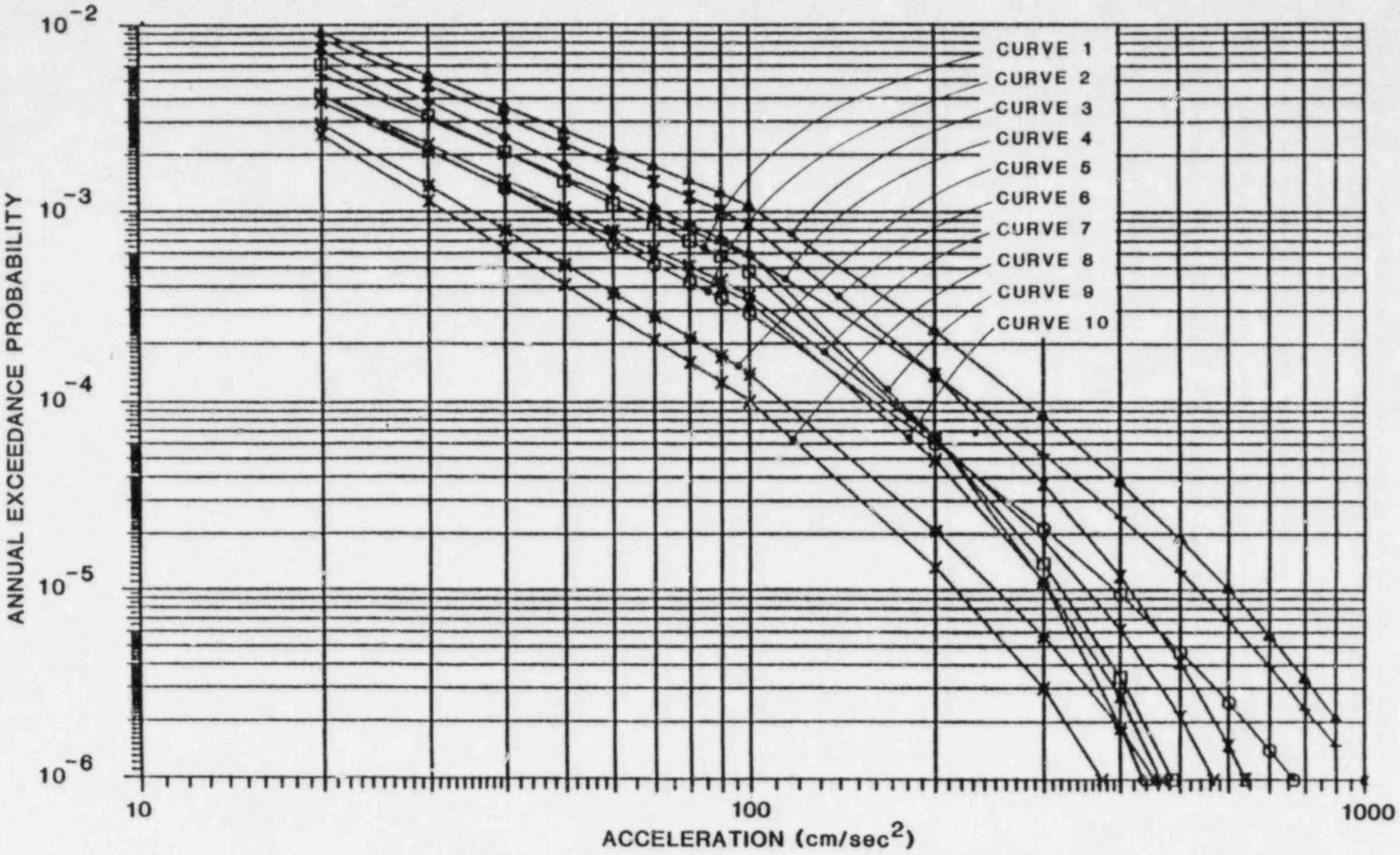

Figure 24

Aggregate Seismic Hazard Curves

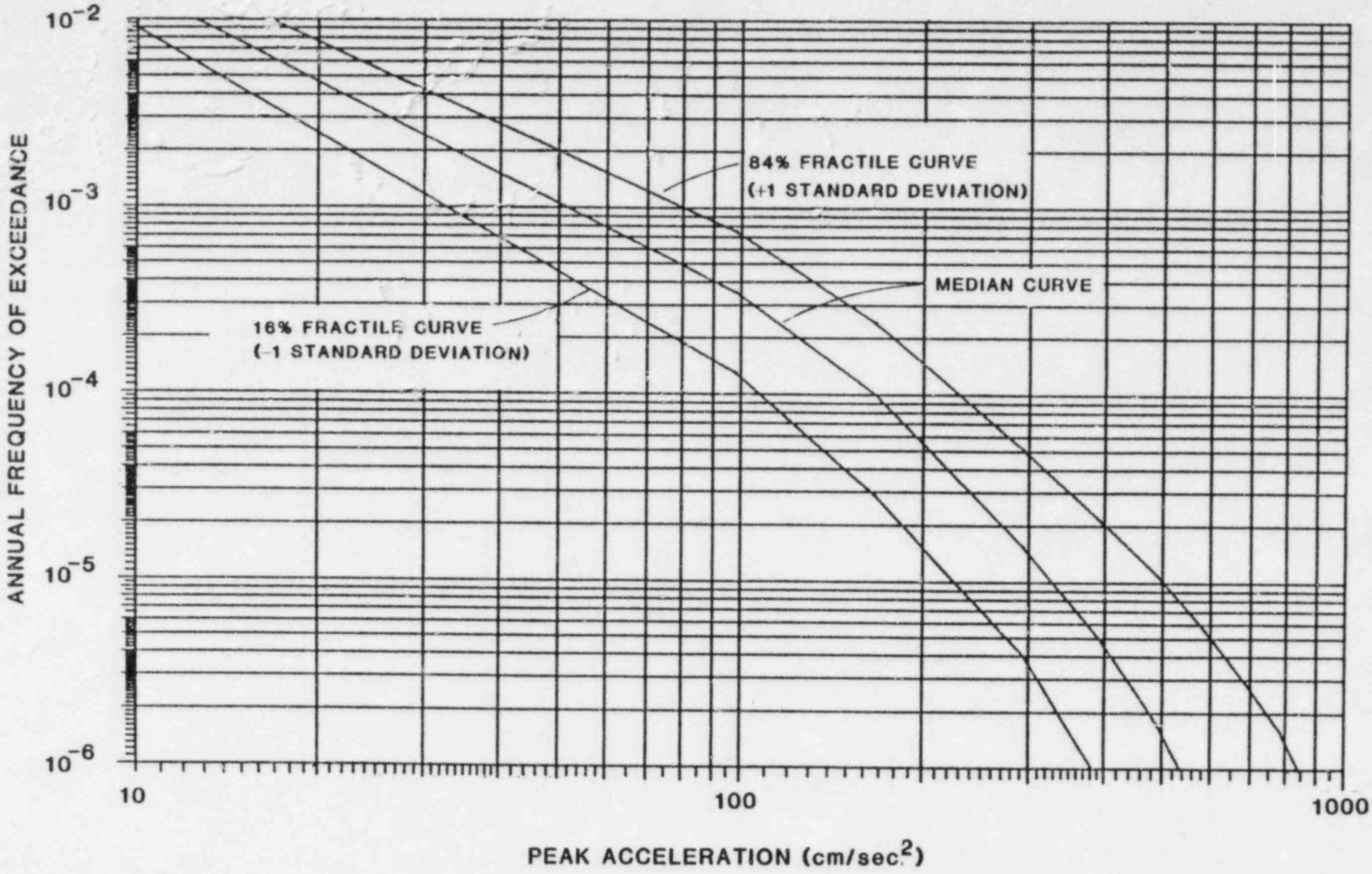

Dames & Moore

Figure 25

Fractile Seismic Hazard Curves

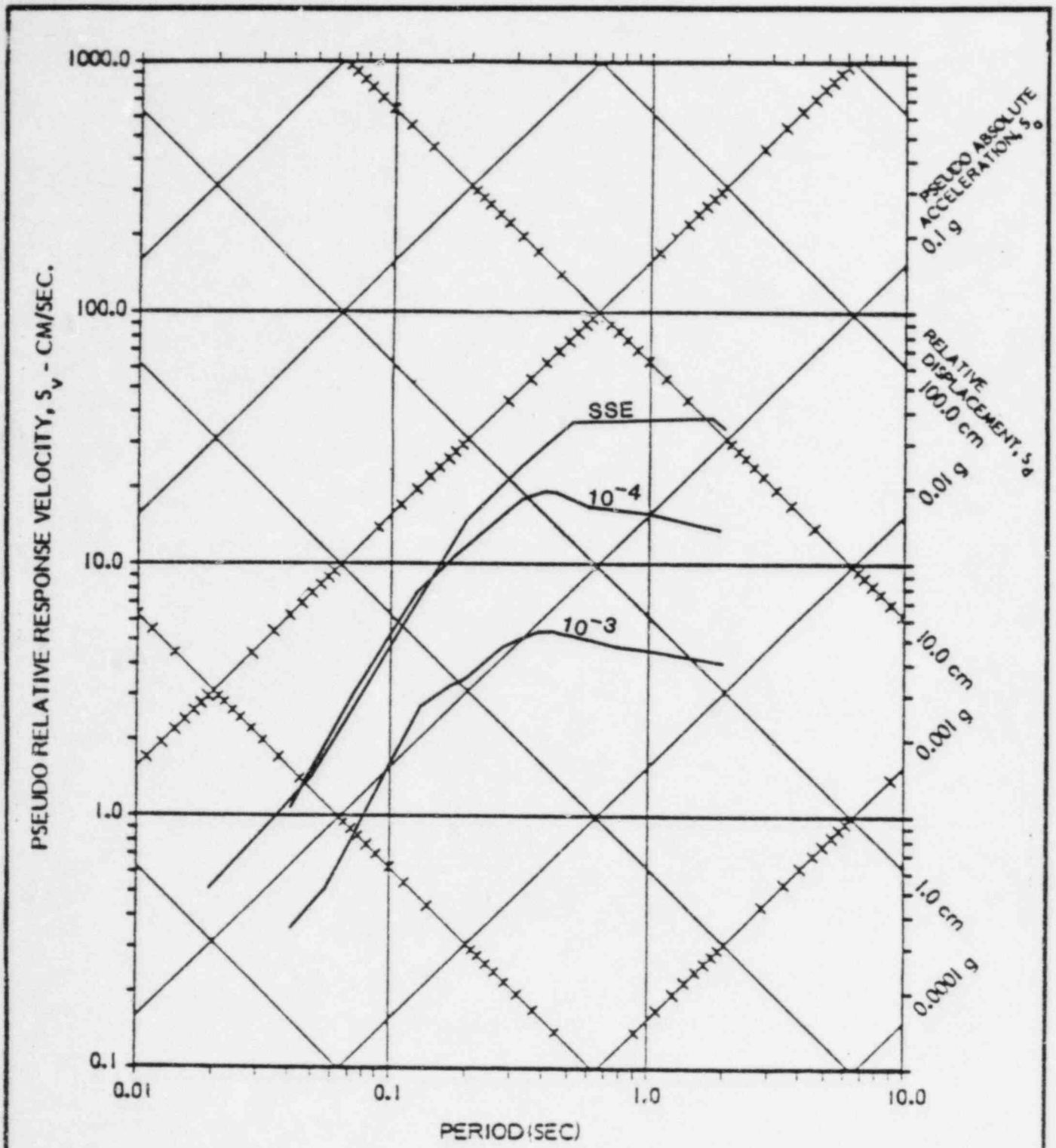

Figure 26

10^{-3} and 10^{-4} Site Spectra Compared to SSE Spectra for Millstone, Unit 3 (5% Damping)

Dames & Moore

APPENDIX A

HISTORICAL SEISMICITY WITHIN
322 km (200 mi) of SITE

(Only events with MM intensity $\geq$ V are listed. Events shown with zero magnitude do not have an independently-determined magnitude.)

DATE	LONG.	LAT.	I_e	m_b	DISTANCE (km)
0 1568	72.50	41.50	6.0	0.0	34.7
0 1574	72.50	41.50	5.0	0.0	34.7
0 1584	72.50	41.50	5.0	0.0	34.7
0 1592	72.50	41.50	5.0	0.0	34.7
0 1627	70.80	42.60	6.0	0.0	182.8
14APR1658	70.90	42.50	5.0	0.0	169.0
10NOV1727	70.60	42.80	7.0	0.0	210.4
19DEC1737	74.00	40.80	7.0	0.0	163.6
14JUN1744	70.90	42.50	6.0	0.0	169.0
18NOV1755	70.30	42.70	8.0	0.0	218.5
12MAR1761	70.90	42.50	5.0	0.0	169.0
30NOV1783	74.50	41.00	6.0	0.0	198.1
16MAY1791	72.50	41.50	6.0	0.0	34.7
10NOV1810	70.80	43.00	5.0	0.0	219.2
29NOV1814	70.30	43.70	5.0	0.0	306.8
5OCT1817	71.20	42.50	6.0	0.0	154.8
23JUL1823	70.60	42.90	5.0	0.0	219.2
12APR1837	72.70	41.70	5.0	0.0	61.9
16JAN1840	75.00	43.00	6.0	0.0	299.6
9AUG1840	72.90	41.50	5.0	0.0	64.4
11NOV1840	75.20	39.80	7.0	0.0	306.1
26OCT1845	73.30	41.20	5.0	0.0	95.3
25AUG1846	70.80	42.50	5.0	0.0	174.3
8AUG1847	70.10	41.70	6.0	0.0	177.7
29SEP1847	74.00	40.50	5.0	0.0	178.2
9SEP1848	74.00	40.40	5.0	0.0	184.2
28NOV1852	70.90	43.00	5.0	0.0	215.1
11DEC1854	70.80	43.00	5.0	0.0	219.2
16JAN1855	71.00	44.00	5.0	0.0	314.0
7FEB1855	74.00	42.00	6.0	0.0	170.3
18NOV1872	71.60	43.20	5.0	0.0	215.3
11DEC1874	73.80	40.90	5.0	0.0	144.0
28JUL1875	73.00	41.90	5.0	0.0	95.2
22SEP1876	71.30	41.50	5.0	0.0	75.6
10SEP1877	74.90	40.30	5.0	0.0	255.8
5FEB1878	73.80	40.00	5.0	0.0	200.3
4OCT1878	74.00	41.50	5.0	0.0	154.1
12MAY1880	71.00	42.70	5.0	0.0	182.3
19DEC1882	71.40	43.20	5.0	0.0	219.5
28FEB1883	71.30	41.50	5.0	0.0	75.6

APPENDIX A (Continued)

DATE	LONG.	LAT.	I_e	m_b	DISTANCE (km)
31MAY1884	75.50	40.60	5.0	0.0	290.6
10AUG1884	74.00	40.60	7.0	0.0	172.8
23NOV1884	71.70	43.20	5.0	0.0	213.7
2MAY1891	71.60	43.20	5.0	0.0	215.3
9MAR1893	74.00	40.60	5.0	0.0	172.8
1SEP1895	74.80	40.70	6.0	0.0	230.9
17MAY1899	72.60	41.60	5.0	0.0	48.2
21JAN1903	70.90	42.10	5.0	0.0	137.2
5MAR1905	72.30	43.60	5.0	0.0	254.9
30AUG1905	70.70	43.10	5.0	0.0	233.0
16OCT1907	71.00	42.80	5.0	0.0	191.8
31MAY1908	75.50	40.60	6.0	0.0	290.6
5JAN1916	73.70	43.70	5.0	0.0	293.9
2FEB1916	74.00	42.90	5.0	0.0	232.5
3FEB1916	74.00	43.00	5.0	0.0	241.0
2NOV1916	73.70	43.30	5.0	0.0	254.5
26JAN1921	75.00	40.00	5.0	0.0	279.7
7JAN1925	70.60	42.60	5.0	0.0	193.5
24APR1925	70.80	41.70	5.0	0.0	122.0
9OCT1925	71.10	43.70	6.0	0.0	279.9
14NOV1925	72.40	41.70	5.0	0.0	47.4
26JAN1926	75.00	40.00	5.0	0.0	279.7
18MAR1926	71.80	42.80	5.0	0.0	168.5
12MAY1926	73.90	40.90	5.0	0.0	152.0
1JUN1927	74.00	40.30	7.0	0.0	190.6
20APR1931	73.70	43.40	7.0	3.8	264.2
25JAN1933	74.70	40.20	5.0	0.0	246.3
10NOV1936	71.40	43.60	5.0	0.0	262.4
23AUG1938	74.50	40.10	5.0	3.5	238.1
15NOV1939	75.20	39.60	5.0	0.0	319.2
28JAN1940	70.80	41.60	5.0	2.6	118.6
20DEC1940	71.30	43.80	7.0	5.5	285.9
3SEP1951	74.30	41.20	5.0	3.4	178.5
25AUG1952	74.50	43.00	5.0	0.0	268.7
8OCT1952	74.00	41.70	5.0	0.0	158.4
27MAR1953	73.50	41.10	5.0	0.0	113.7
31MAR1953	73.00	43.70	5.0	3.1	274.3
21FEB1954	75.90	41.20	7.0	0.0	312.0
29JUL1954	70.70	42.70	5.0	3.1	196.6
21JAN1955	73.70	43.00	5.0	0.0	226.3
23MAR1957	74.80	40.60	6.0	3.7	234.5
26APR1957	69.80	43.60	6.0	4.8	320.4

APPENDIX A (Concluded)

DATE	LONG.	LAT.	I_e	m_b	DISTANCE (km)
19SEP1958	70.20	43.60	5.0	0.0	301.6
15SEP1961	75.50	40.80	5.0	0.0	284.9
27DEC1961	74.80	40.50	5.0	0.0	238.7
29DEC1962	71.70	42.80	5.0	0.0	170.2
16OCT1963	70.40	42.50	5.0	3.3	197.4
26JUN1964	71.50	43.30	5.0	3.5	228.0
17NOV1964	73.70	41.20	5.0	0.0	128.5
24OCT1965	70.10	41.30	5.0	0.0	172.9
2FEB1967	71.20	41.60	5.0	3.1	87.0
22NOV1967	73.80	41.20	5.0	0.0	136.8
3NOV1968	72.50	41.40	5.0	3.3	29.3
10DEC1968	74.60	39.70	5.0	2.5	272.5
6AUG1969	71.40	43.80	5.0	2.6	284.0
21OCT1971	71.20	42.70	5.0	2.3	174.1
7JUN1974	73.90	41.60	6.0	3.3	147.7
11MAR1976	71.20	41.60	5.0	2.9	87.0
11MAR1976	74.40	41.00	5.0	2.4	189.9
14MAR1976	70.00	41.70	5.0	2.8	185.8
13APR1976	74.00	40.80	6.0	3.1	163.6